

Higgs Boson Pair Production @ NLO in QCD



Max-Planck-Institut für Physik
(Werner-Heisenberg-Institut)

Stephen Jones

Borowka, Greiner, Heinrich, Kerner, Schlenk, Schubert, Zirke

JHEP (2016) 107

PRL 117 (2016) 012001, Erratum 079901

PoS LL2016 (2016) 069



MAX-PLANCK-GESELLSCHAFT



Motivation

Higgs Lagrangian:

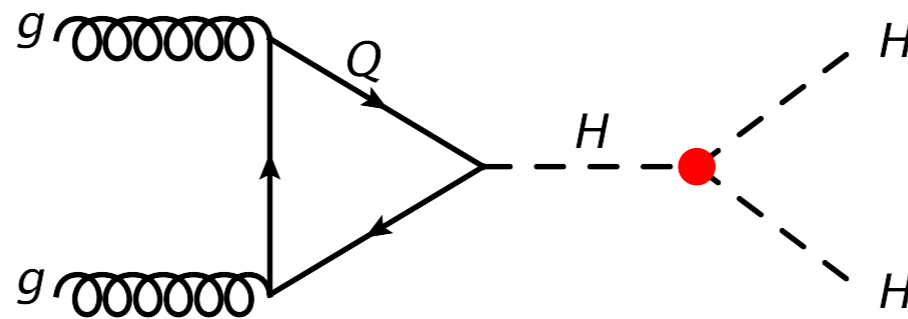
$$\mathcal{L} \supset -V(\Phi^\dagger\Phi), \quad V(\Phi^\dagger\Phi) = -\frac{1}{2}\mu^2\Phi^\dagger\Phi + \frac{1}{4}\lambda(\Phi^\dagger\Phi)^2$$



EW symmetry breaking

$$\frac{m_H^2}{2}H^2 + \boxed{\frac{m_H^2}{2v}H^3} + \frac{m_H^2}{8v^2}H^4$$

Higgs pair production probes triple-Higgs coupling



Production Channels

$$\sigma(pp \rightarrow HH + X) @ 14 \text{ TeV}$$

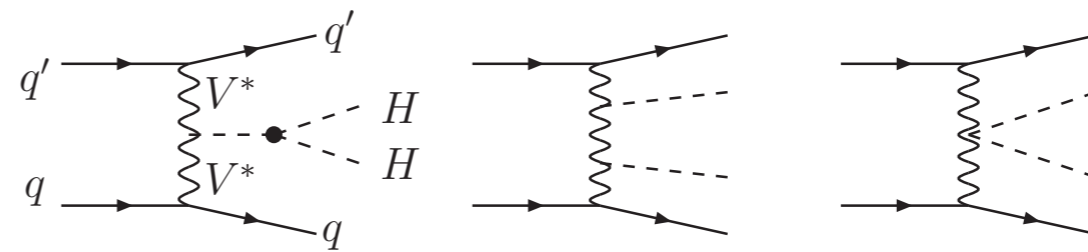
Gluon Fusion



Vector Boson Fusion (VBF)

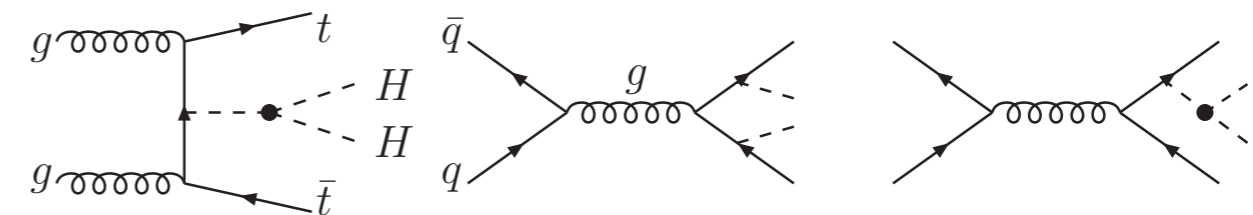
NLO [1,2] NNLO [3]

+ non-negligible contribution
from $gg \rightarrow HHjj$ LO [5]



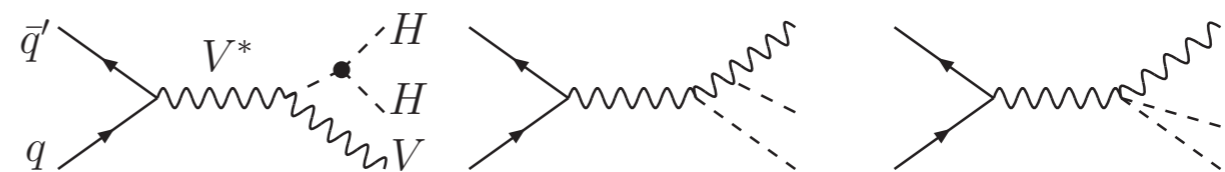
Top-Quark Associated

NLO [2]



Higgs-strahlung

NLO [1,2] NNLO [1,4]



[1] Baglio, Djouadi, Gröber, Mühlleitner, Quevillon, Spira 12;

[2] Frederix, Frixione, Hirschi, Maltoni, Mattelaer, Torrielli, Vryonidou, Zaro 14;

[3] Ling, Zhang, Ma, Guo, Li, Li 14 [4] Li, Wang 16

[5] Dolan, Englert, Greiner, Nordstrom, Spannowsky 15;

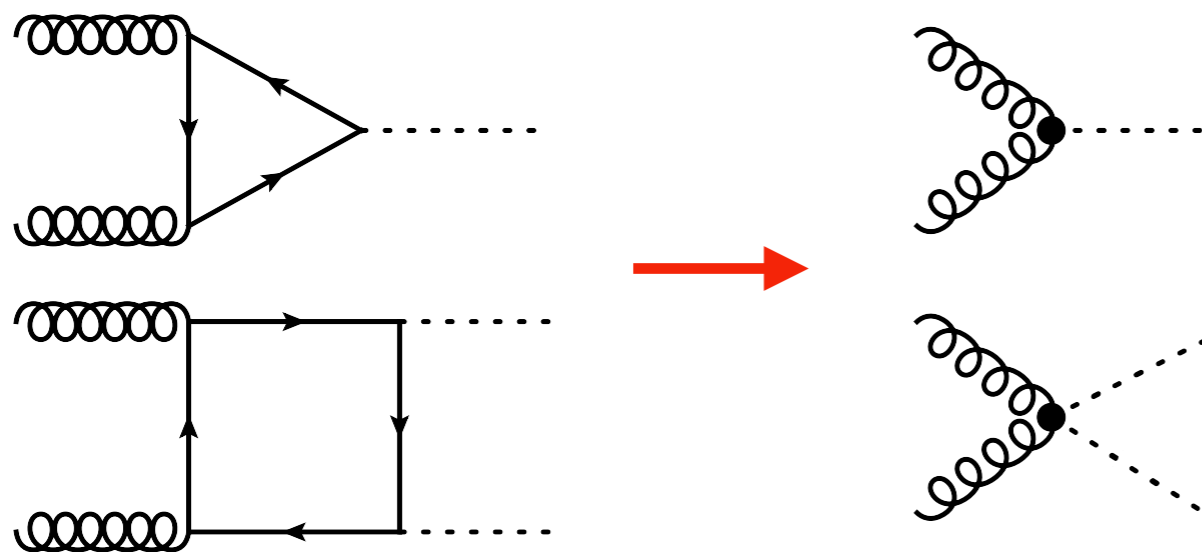
Baglio, Djouadi et al. 12

Higgs EFT

H(iggs)EFT: $m_T \rightarrow \infty$

Effective tree-level couplings between gluons and Higgs

Lowers number of loops by 1



HEFT valid for

$$\sqrt{\hat{s}} \ll 2m_T$$

HH production for

$$2m_H < \sqrt{\hat{s}}$$

Small energy range in which HEFT is technically justified

Born improved NLO HEFT:

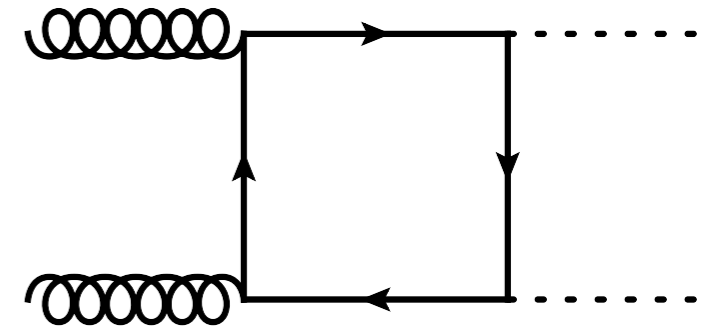
$$d\sigma_{\text{NLO}}(m_T) \approx d\bar{\sigma}_{\text{NLO}}(m_T) \equiv \frac{d\sigma_{\text{NLO}}(m_T \rightarrow \infty)}{d\sigma_{\text{LO}}(m_T \rightarrow \infty)} d\sigma_{\text{LO}}(m_T)$$

Spira et al. (HPAIR)

Gluon Fusion

1. LO (1-loop), Dominated by top (bottom <1%)

Glover, van der Bij 88



2. Born Improved NLO H(iggs)EFT $m_T \rightarrow \infty$ **$K \approx 2$**

Dawson, Dittmaier, Spira 98

- A. Including m_T in Real radiation

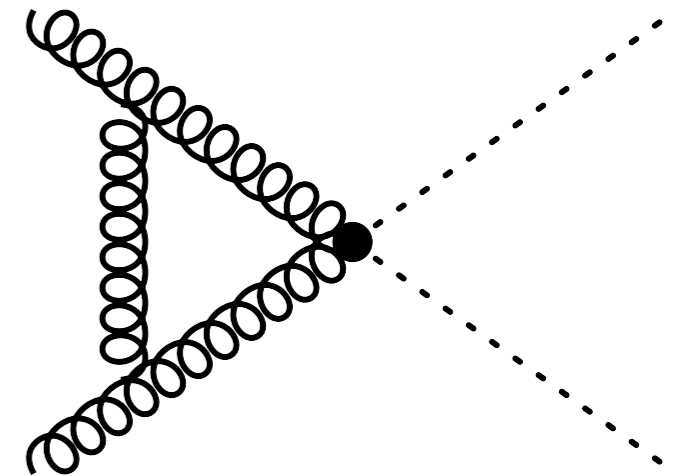
-10%

Maltoni, Vryonidou, Zaro 14

- B. Including $\mathcal{O}(1/m_T^{12})$ terms in Virtual MEs **$\pm 10\%$**

Grigo, Hoff, Melnikov, Steinhauser 13; Grigo, Hoff 14;

Grigo, Hoff, Steinhauser 15



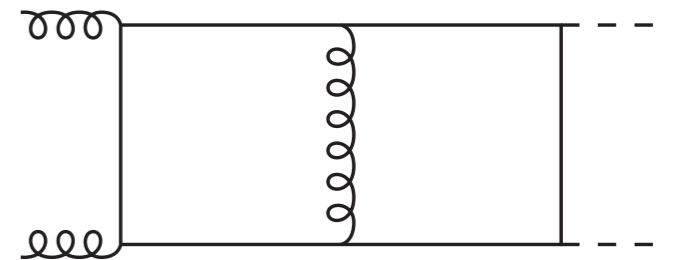
3. NLO (2-loop) with full top mass **← this talk**

Borowka, Greiner, Heinrich, SPJ, Kerner, Schlenk, Schubert, Zirke 16;

Borowka, Greiner, Heinrich, SPJ, Kerner, Schlenk, Zirke 16

(Transverse momentum) NLL + NLO

Ferrera, Pires 16



Gluon Fusion (II)

4. Born Improved NNLO HEFT

De Florian, Mazzitelli 13

+20%

Including matching coefficients

Grigo, Melnikov, Steinhauser 14

Including terms $\mathcal{O}(1/m_T^4)$ in Virtual MEs

Grigo, Hoff, Steinhauser 15

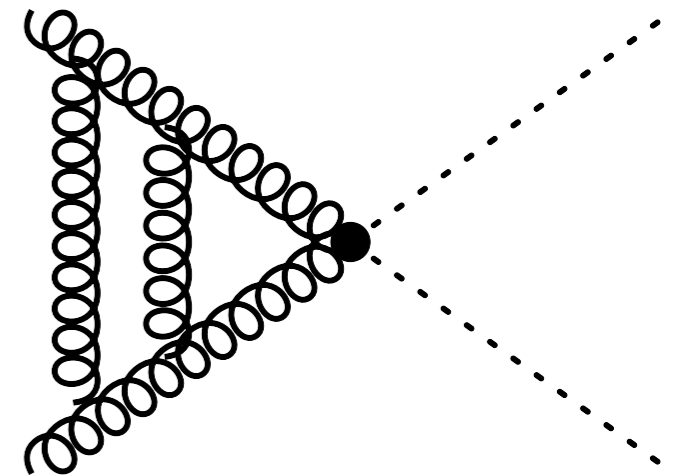
(Threshold) NNLL + NNLO Matching

(SCET) Shao, Li, Li, Wang 13; de Florian, Mazzitelli 15

+9%

5. NNLO HEFT (Differential)

de Florian, Grazzini, Hanga, Kallweit, Lindert, Maierhöfer,
Mazzitelli, Rathlev 16

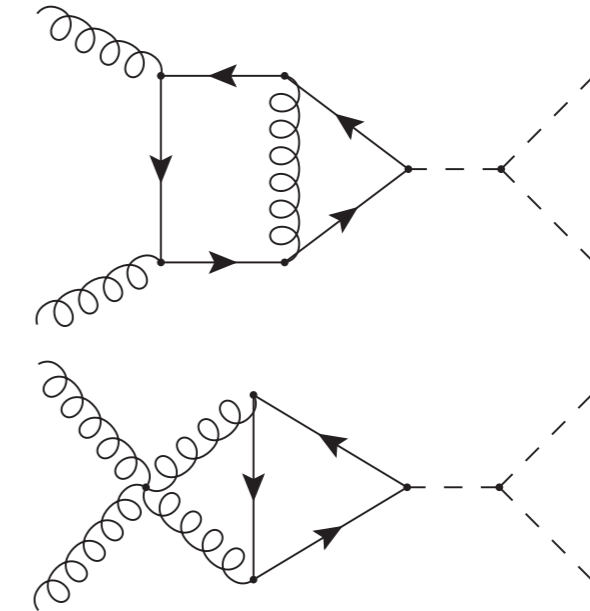
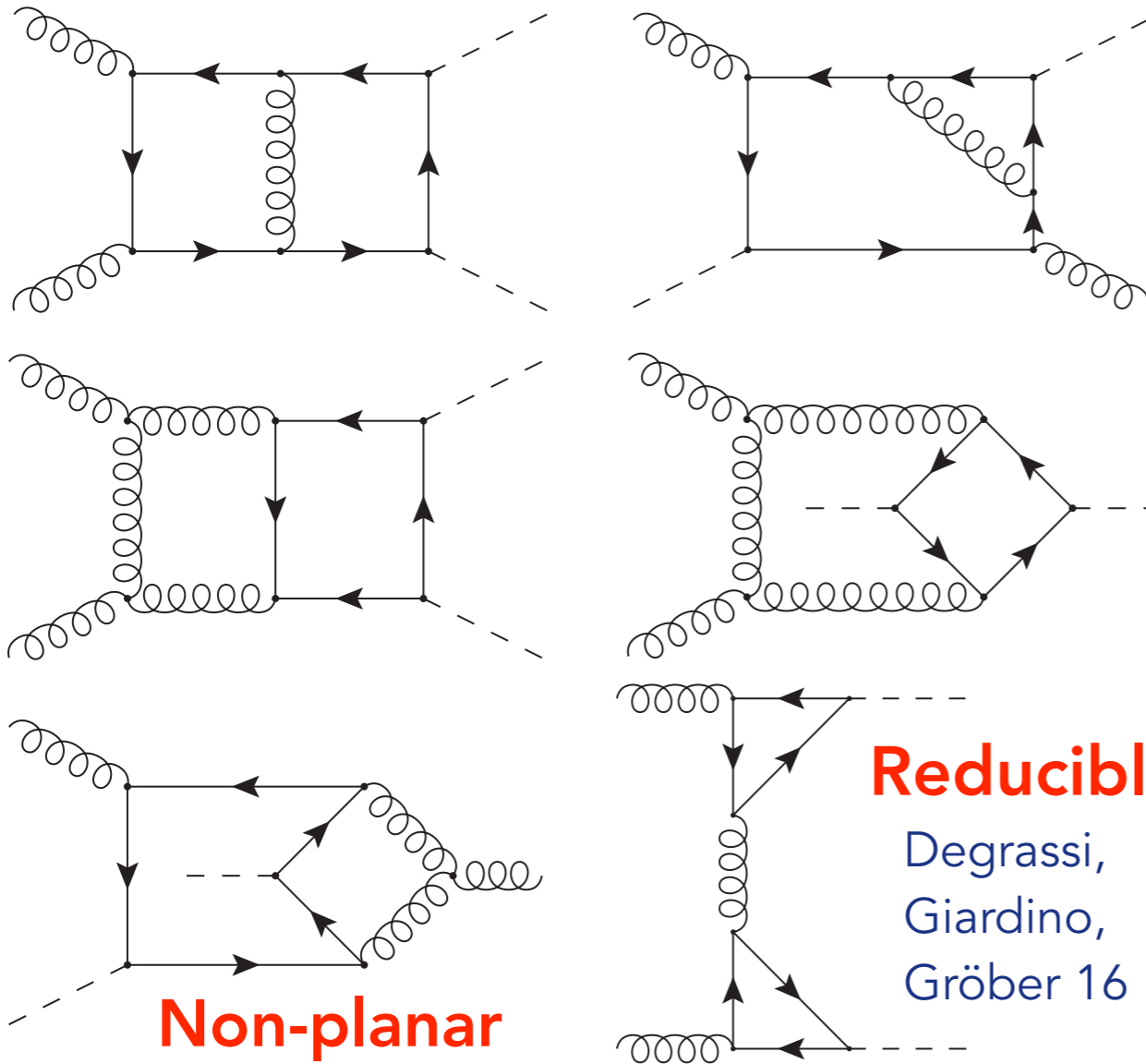


NLO Calculation

Virtual MEs: $gg \rightarrow HH$ ~~$q\bar{q} \rightarrow HH$~~ ← **NNLO**

Yukawa only (≤ 4 -point)

Self-coupling (≤ 3 -point)



Integrals Known

$gg \rightarrow H$

Spira, Djouadi et al. 93, 95;
 Bonciani, P. Mastrolia 03,04;
 Anastasiou, Beerli et al. 06;

Many integrals not known analytically, except:

$H \rightarrow Z\gamma$ Bonciani, Del Duca, Frellesvig et al. 15; Gehrmann, Guns, Kara 15;

Form Factor Decomposition

Expose tensor structure: $\mathcal{M} = \epsilon_{\mu}^1 \epsilon_{\nu}^2 \mathcal{M}^{\mu\nu}$

Form Factors (Contain integrals)

$$\mathcal{M}^{\mu\nu} = F_1(\hat{s}, \hat{t}, m_h^2, m_t^2, D) T_1^{\mu\nu} + F_2(\hat{s}, \hat{t}, m_h^2, m_t^2, D) T_2^{\mu\nu}$$

(Tensor) Basis, built from external momenta & metric

Choose: $\mathcal{M}^{++} = \mathcal{M}^{--} = -F_1$

$\mathcal{M}^{+-} = \mathcal{M}^{-+} = -F_2$

Glover, van der Bij 88

Construct projectors such that:

$$P_1^{\mu\nu} \mathcal{M}_{\mu\nu} = F_1(\hat{s}, \hat{t}, m_h^2, m_t^2, D)$$

$$P_2^{\mu\nu} \mathcal{M}_{\mu\nu} = F_2(\hat{s}, \hat{t}, m_h^2, m_t^2, D)$$

Integral Reduction

Tensor integrals rewritten as inverse propagators

Scalar products:

$$S = \frac{l(l+1)}{2} + lm$$

$l = 2$ # Loops

$m = 3$ # L.I External momenta

$$S = 9$$

4 scales $\hat{s}, \hat{t}, m_T^2, m_H^2$

Choose 5 planar + 3 non-planar integral families

Integrals	1-loop	2-loop
Direct	63	9865
+ Symmetries	21	1601
+ IBPs	8	~260-270 (currently 327)

Reduction with REDUZE 2

von Manteuffel, Studerus 12

Up to 4 inverse propagators

Simplification, fix:

$$m_T = 173 \text{ GeV}, m_H = 125 \text{ GeV}$$

(Mostly) Finite Basis

Panzer 14; von Manteuffel, Panzer, Schabinger 15

Non-planar integrals computed mostly **without reduction**

Amplitude Evaluation

All master integrals processed with SecDec

Borowka, Heinrich, Jahn, SJ, Kerner, Schlenk, Zirke

Sector decompose Feynman integrals Hepp 66; Denner, Roth 96; Binoth, Heinrich 00

Contour deformation Soper 00; Binoth, Guillet, Heinrich et al. 05; Nagy, Soper 06; Borowka et al. 12

Use Quasi-Monte-Carlo (QMC) integration $\mathcal{O}(n^{-1})$ error scaling

Review: Dick, Kuo, Sloan 13; Li, Wang, Yan, Zhao 15

Implemented in OpenCL, evaluated on GPUs

Entire 2-loop amplitude evaluated with a single code

$$F = \sum_i \left(\sum_j C_{i,j} \epsilon^j \right) \left(\sum_k I_{i,k} \epsilon^k \right) = \epsilon^{-2} \left[C_{1,-2}^{(L)} I_{1,0}^{(L)} + \dots \right] + \epsilon^{-1} \left[C_{1,-1}^{(L)} I_{1,0}^{(L)} + \dots \right] + \dots$$

compute once

Dynamically set target precision for each sector, minimising time:

$$T = \sum_i t_i + \bar{\lambda} \left(\sigma^2 - \sum_i \sigma_i^2 \right), \quad \sigma_i \sim t_i^{-e}$$

$\bar{\lambda}$ – Lagrange multiplier

σ – precision goal

σ_i – error estimate

Phase-space Sampling

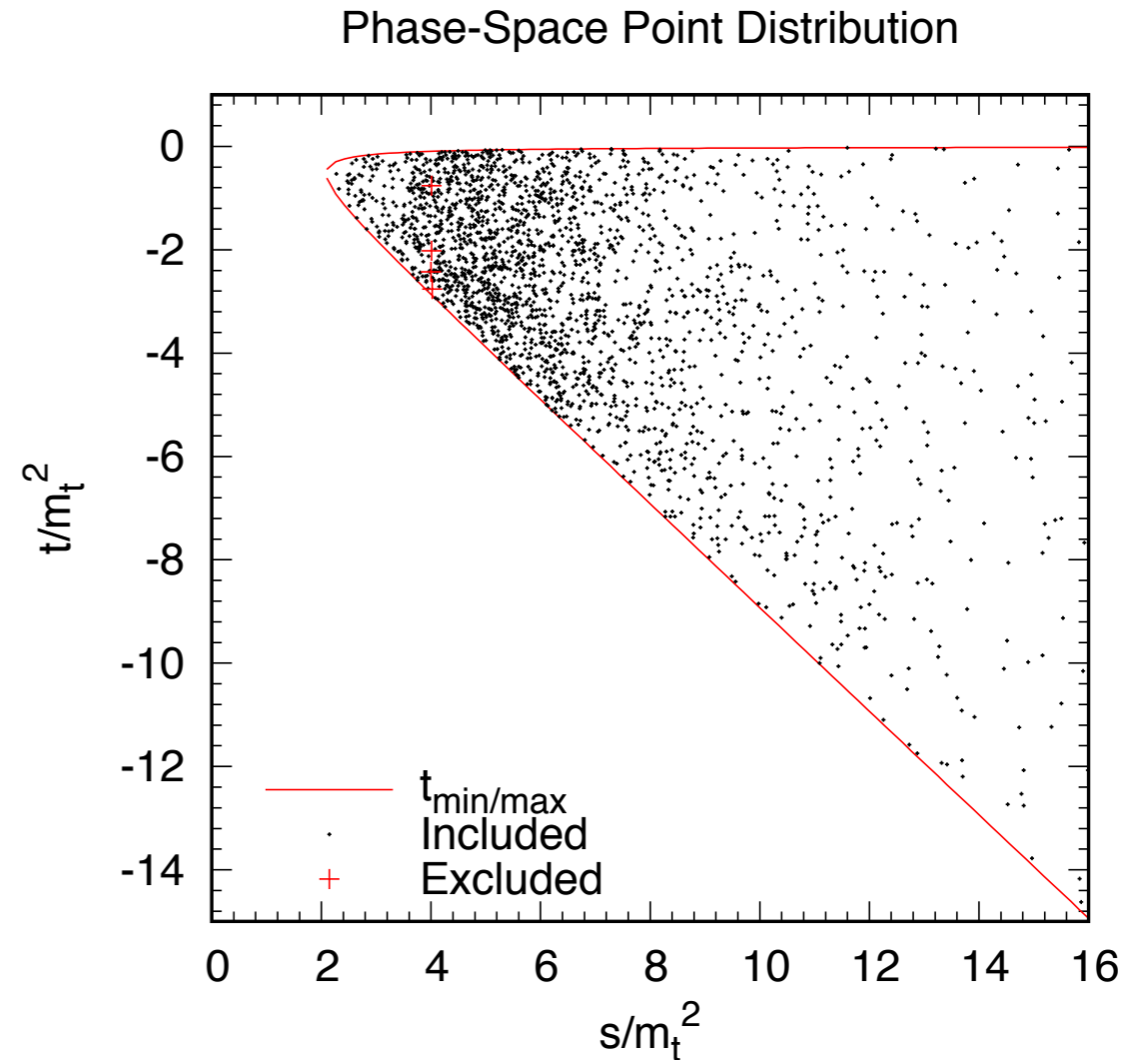
- 1) VEGAS algorithm applied to LO calculation; $\mathcal{O}(100k)$ events computed
- 2) unweighted LO events using accept/reject method; $\mathcal{O}(30k)$ events remain
- 3) Randomly select 917+150 events, compute at NLO, exclude 4+1

Accuracy goal: 3% for F_1

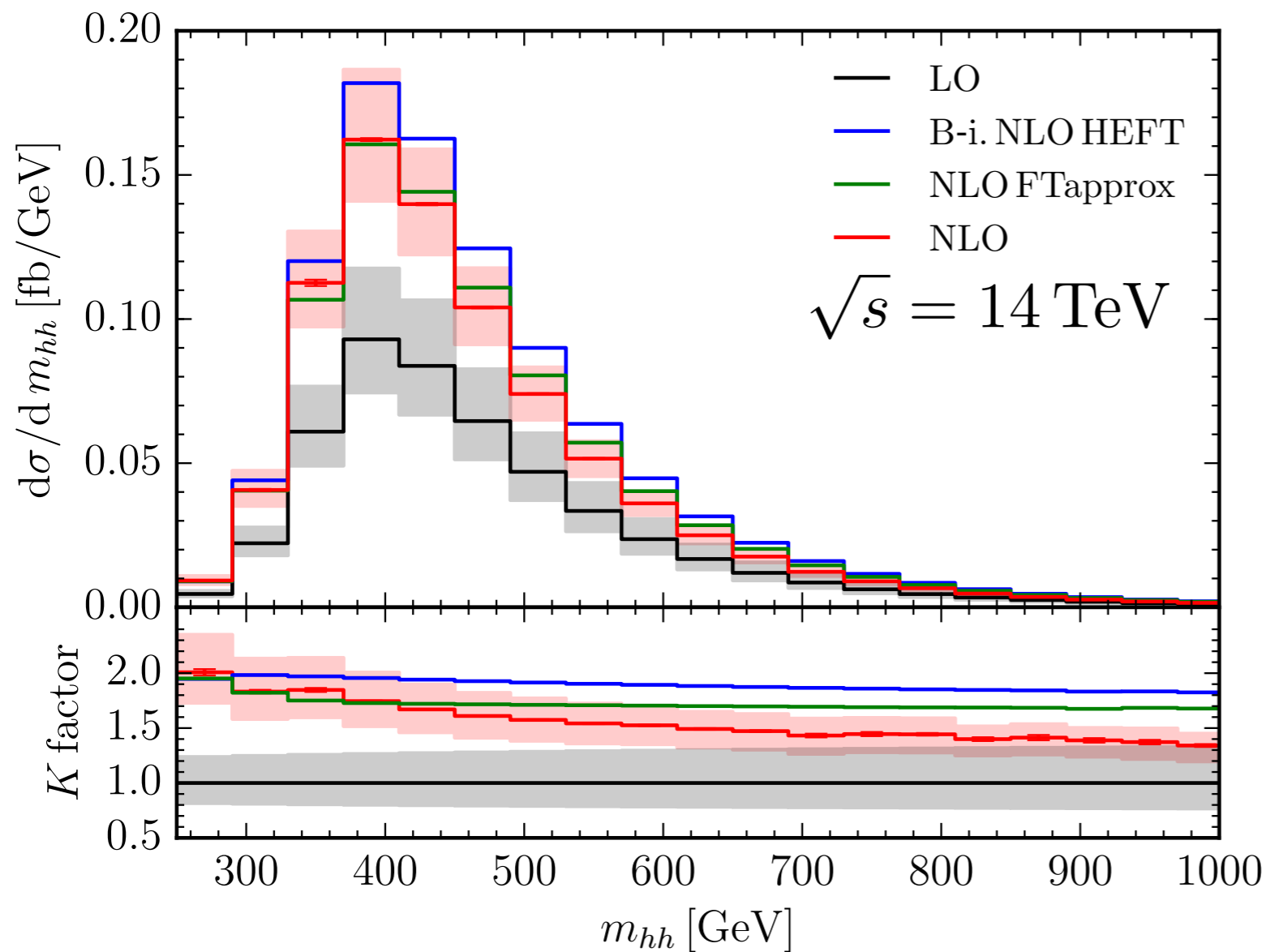
5-20% for F_2 (depending on F_2/F_1)

GPU Time/PS point: 80 min - 2 d (=wall-clock limit)
median 2 h

Additional 1488 events now on disk (not used yet)



Results: Invariant Mass



PDF4LHC15_nlo_30_pdfas

$m_H = 125$ GeV

$m_T = 173$ GeV

Uncertainty:

$$\mu_0 = \frac{m_{HH}}{2}$$

$$\mu_{R,F} \in \left[\frac{\mu_0}{2}, 2\mu_0 \right] \quad (7\text{-point})$$

HEFT: Outside scale var.

$$m_{hh} > 420 \text{ GeV}$$

FTapp: Outside scale var.

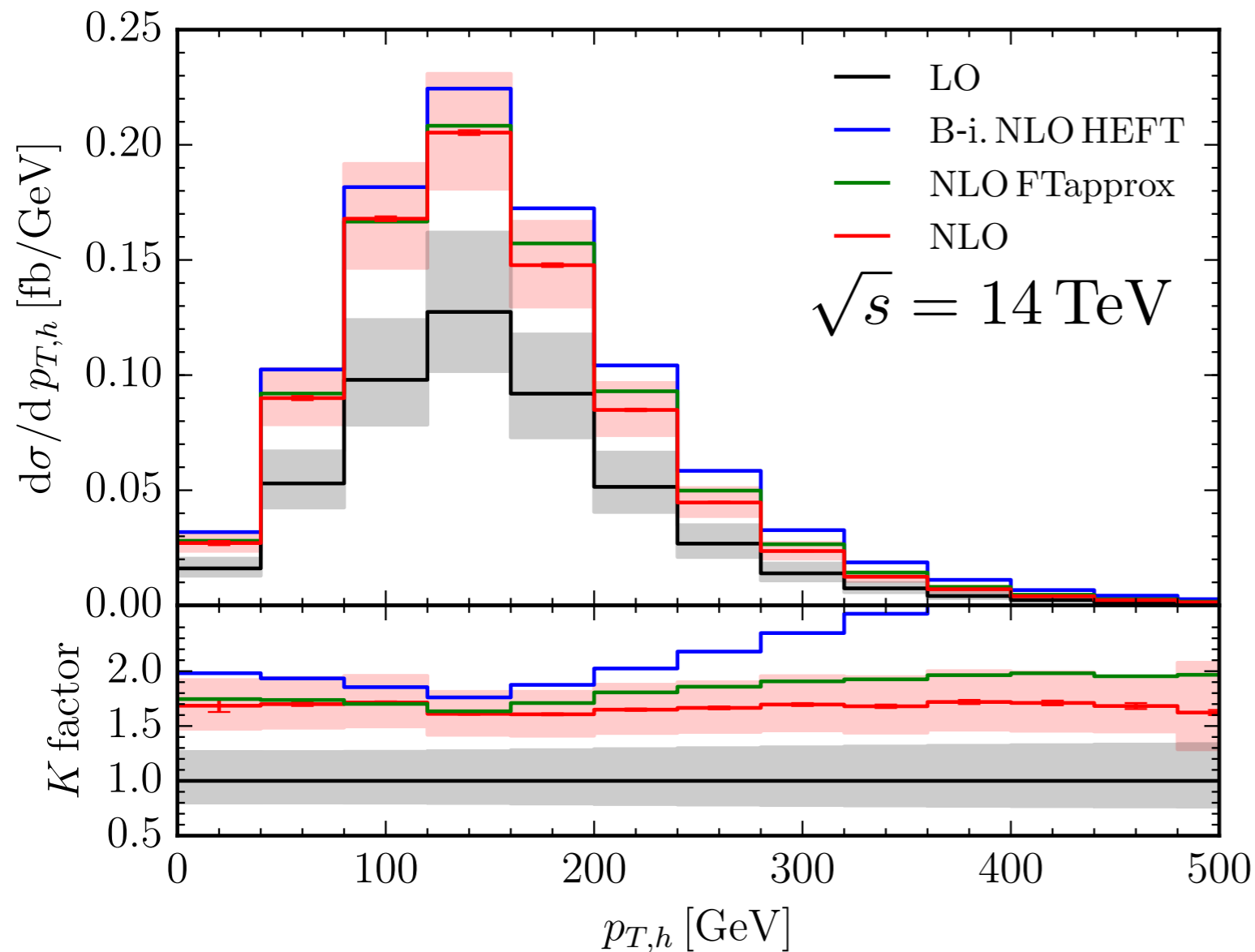
$$m_{hh} > 620 \text{ GeV}$$

	σ_{LO} (fb)	σ_{NLO} (fb)
B.I. HEFT	$19.85^{+27.6\%}_{-20.5\%}$	$38.32^{+18.1\%}_{-14.9\%}$
FTapprox	$19.85^{+27.6\%}_{-20.5\%}$	$34.26^{+14.7\%}_{-13.2\%}$
Full Theory	$19.85^{+27.6\%}_{-20.5\%}$	$32.91^{+13.6\%}_{-12.6\%} \pm 0.3\%$(stat.) $\pm 0.1\%$(int.)

HEFT overestimates by 16%

FTapp. overestimates by 4%

Results: p_T either Higgs



HEFT: Can poor approx.
for larger $p_{T,h}$

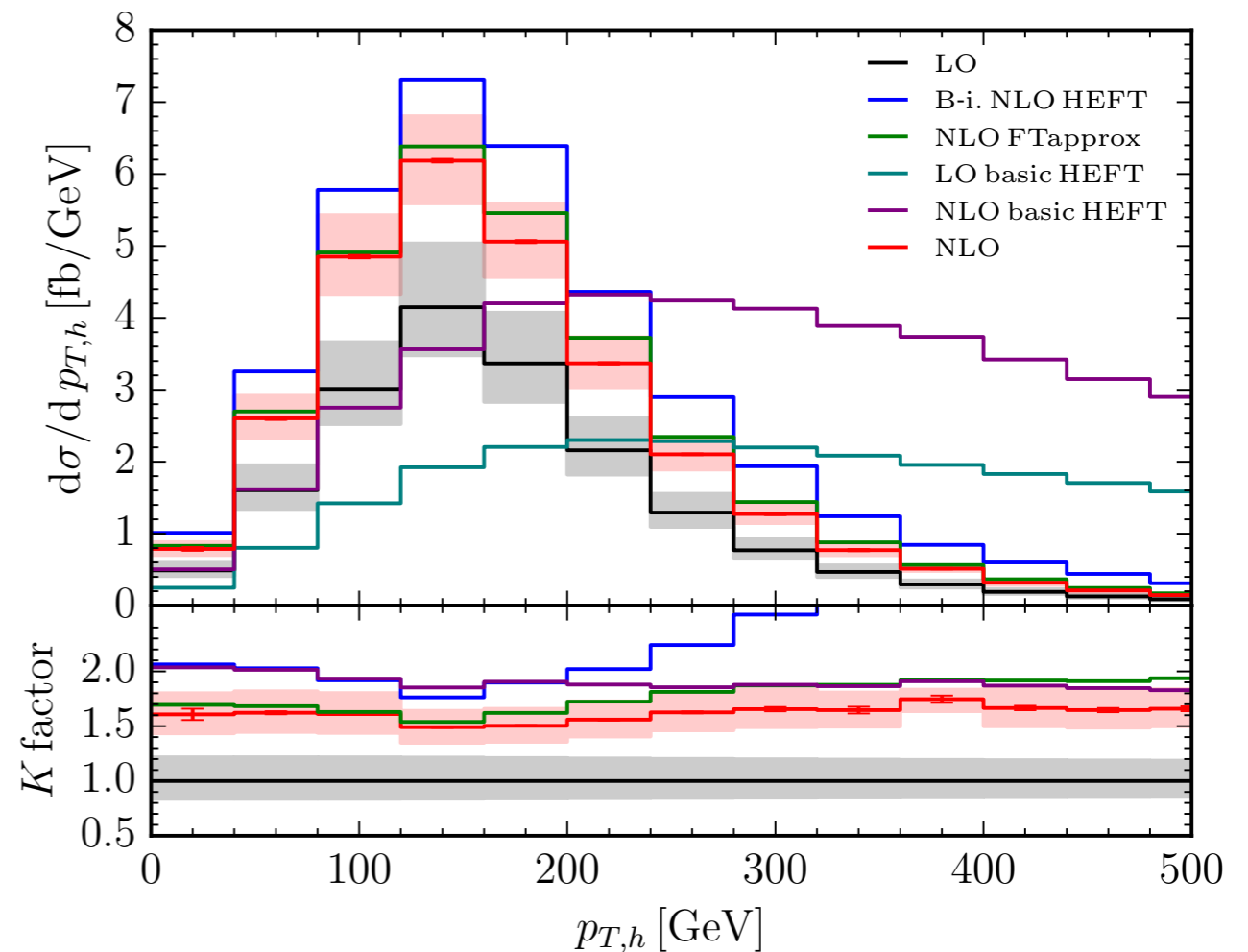
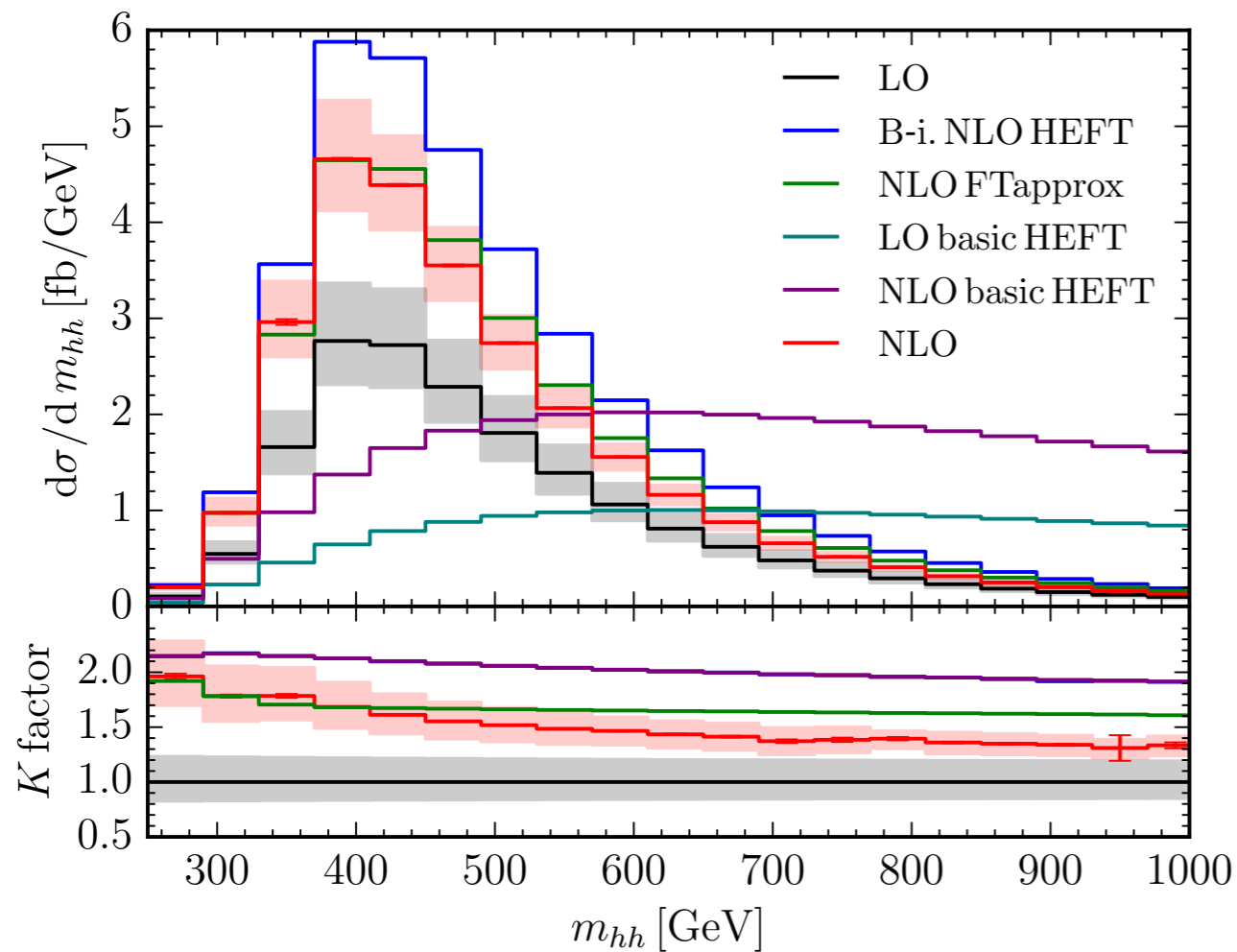
Note: ambiguous how to
rescale HEFT reals by full
LO born differentially

FTapp: Significantly better
but still overestimating

Real radiation plays larger role for large $p_{T,h}$

(As hoped) Including full reals does improve over HEFT in tails

Results: 100TeV



	σ_{LO} (fb)	σ_{NLO} (fb)
B.I. HEFT	—	$1511^{+16.0\%}_{-13.0\%}$
FTapprox	—	$1220^{+11.9\%}_{-10.7\%}$
Full Theory	$731.3^{+20.9\%}_{-15.9\%}$	$1149^{+10.8\%}_{-10.0\%}$

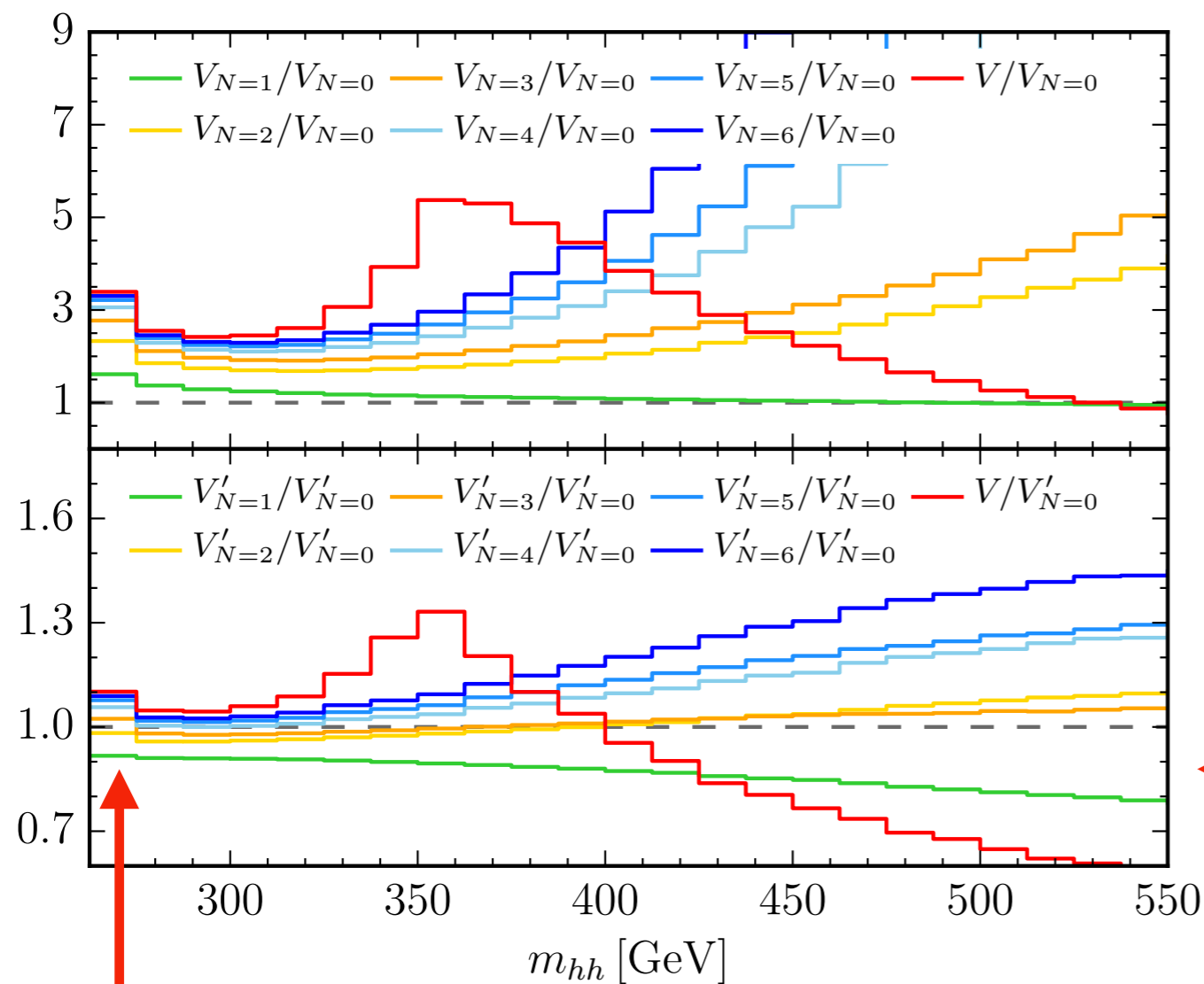
HEFT overestimates by 32%
FTap. overestimates by 6%

Difference between full theory and HEFT more pronounced

Comparison to Expansion

Can compare just virtual ME to expansion:

$$d\hat{\sigma}_N = \sum_{\rho=0}^N d\hat{\sigma}^{(\rho)} \left(\frac{\Lambda}{m_t} \right)^{2\rho} \quad \Lambda \in \left\{ \sqrt{\hat{s}}, \sqrt{\hat{t}}, \sqrt{\hat{u}}, m_h \right\}$$



$$V_N = (d\hat{\sigma}_N^V + d\hat{\sigma}_N^{LO} \otimes \mathbf{I})$$

$$V'_N = V_N \frac{d\hat{\sigma}^{LO}}{d\hat{\sigma}_N^{LO}}$$

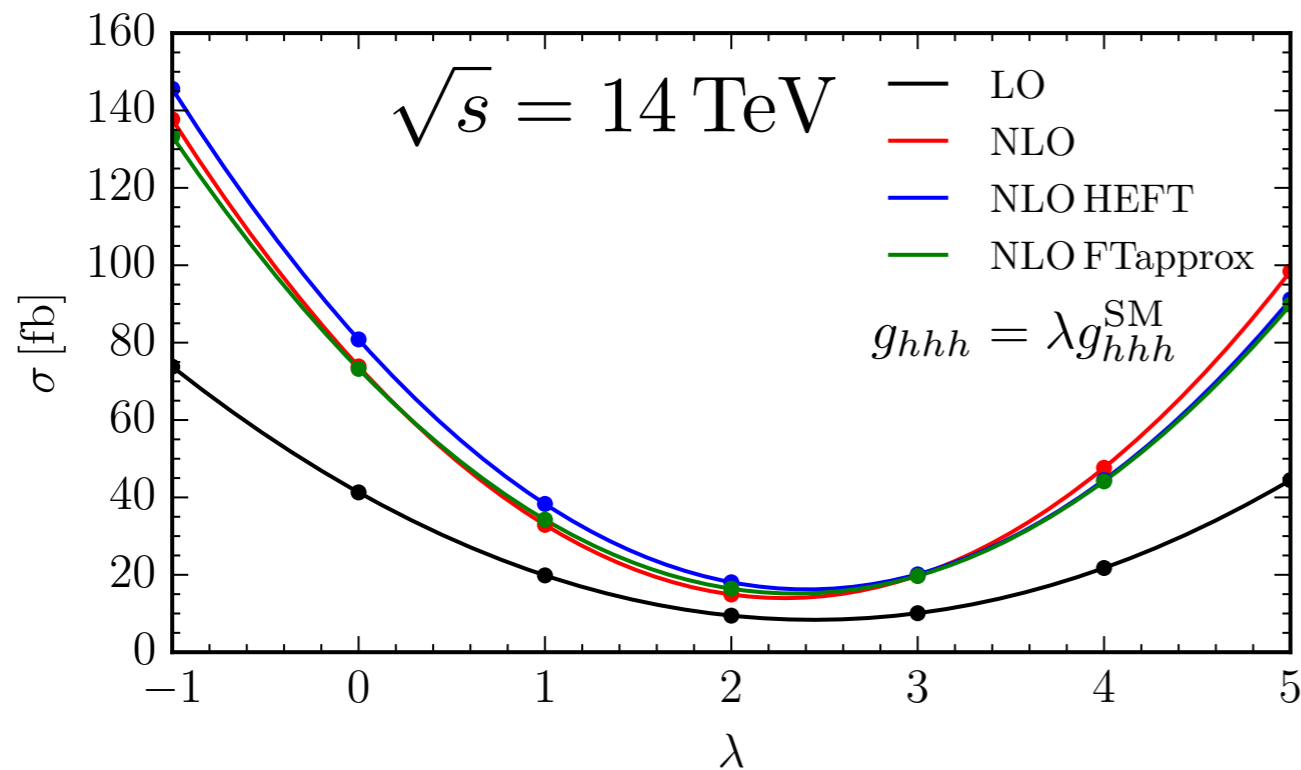
Rescaled better but
does not describe full
above threshold

Expansion converges on full $\sqrt{\hat{s}} < 2m_T$

$V_{N \geq 4}$ thanks to J. Hoff
Grigo, Hoff, Steinhauser 15

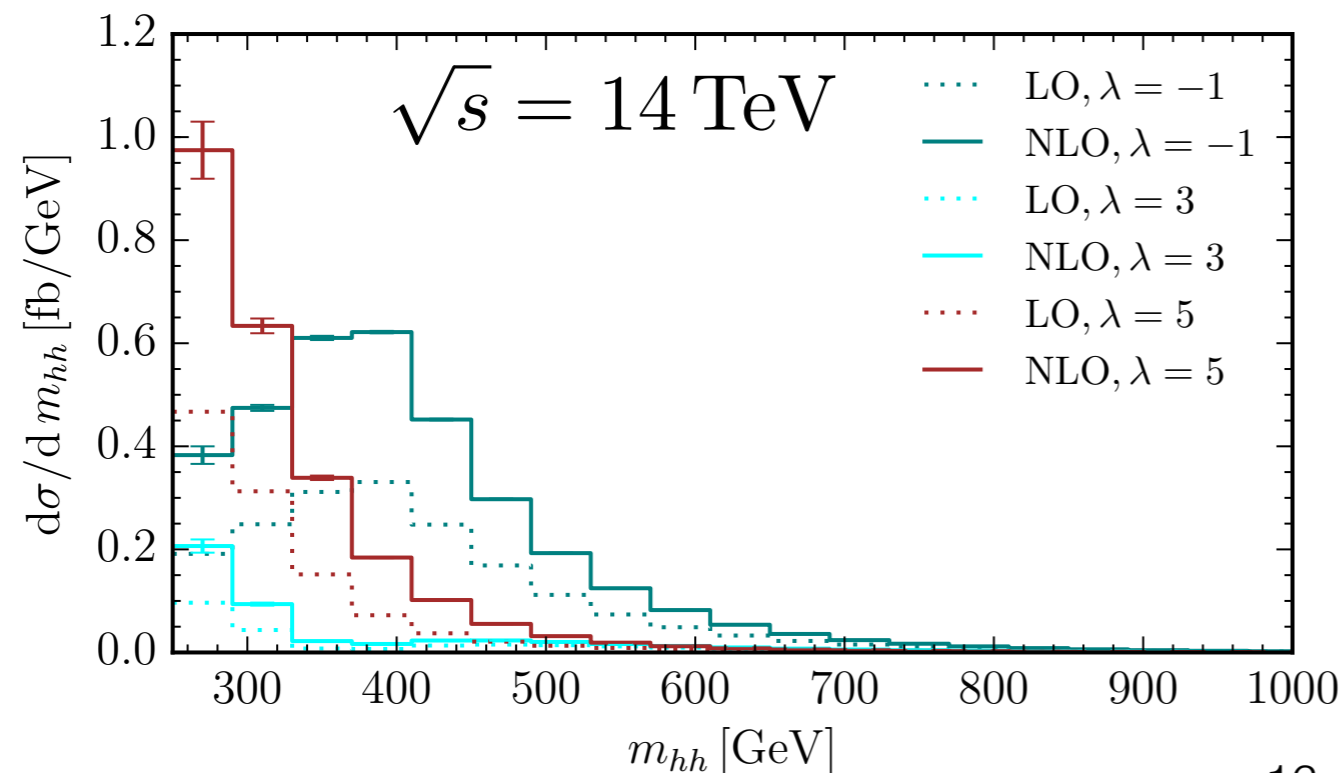
Triple-Higgs Coupling Sensitivity

Note: Just varying λ : one "direction" in EFT parameter space



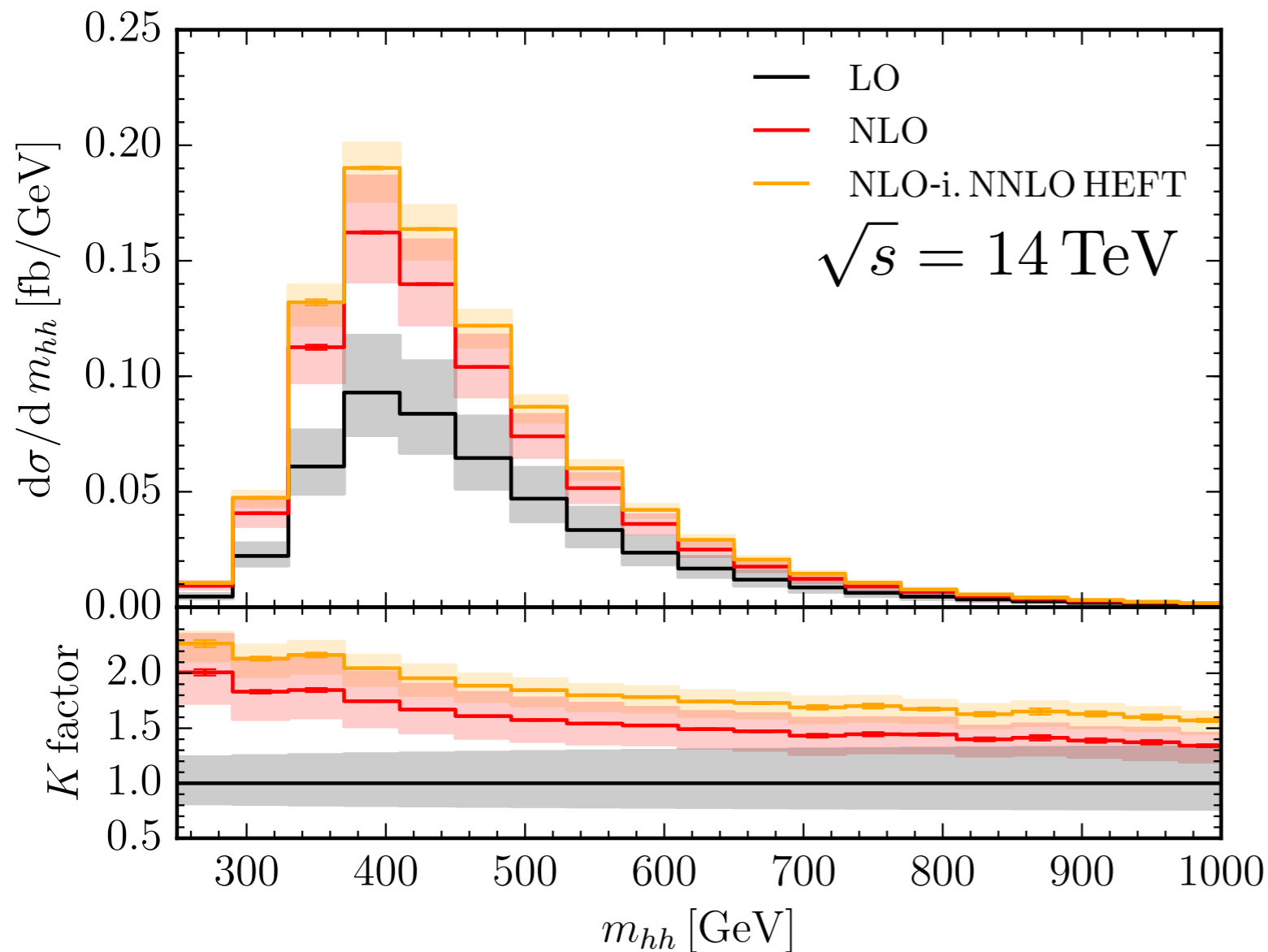
SM: Destructive interference between g_{hhh} and y_T^2 contrib.

Quadratic dependence on λ (at LO in λ)



Distributions: can help to distinguish between λ values that give same total cross-section

NLO Improved NNLO HEFT



First attempt to combine full NLO

Borowka, Greiner, Heinrich, SPJ, Kerner, Schlenk, Zirke 16

+

NNLO HEFT (Differential)

de Florian, Grazzini, Hanga, Kallweit, Lindert, Maierhöfer, Mazzitelli, Rathlev 16

$$\frac{d\sigma^{\text{approx.}}}{dm_{hh}} \equiv \frac{d\sigma_{\text{NLO}}}{dm_{hh}} \times \frac{d\sigma_{\text{NNLO HEFT}}^{\text{HEFT}}/dm_{hh}}{d\sigma_{\text{NLO}}^{\text{HEFT}}/dm_{hh}}$$

Bin-by-bin rescaling of NLO by NNLO HEFT K-factor

$$\sigma^{\text{approx.}} = 38.67^{+5.2\%}_{-7.6\%}$$

Conclusion

Gluon Fusion

- Key measurement for probing the self coupling (HL-LHC era)
- NLO deviates from Born Improved HEFT
 - 14% @ 14 TeV, -24% @ 100 TeV
- Distributions altered significantly

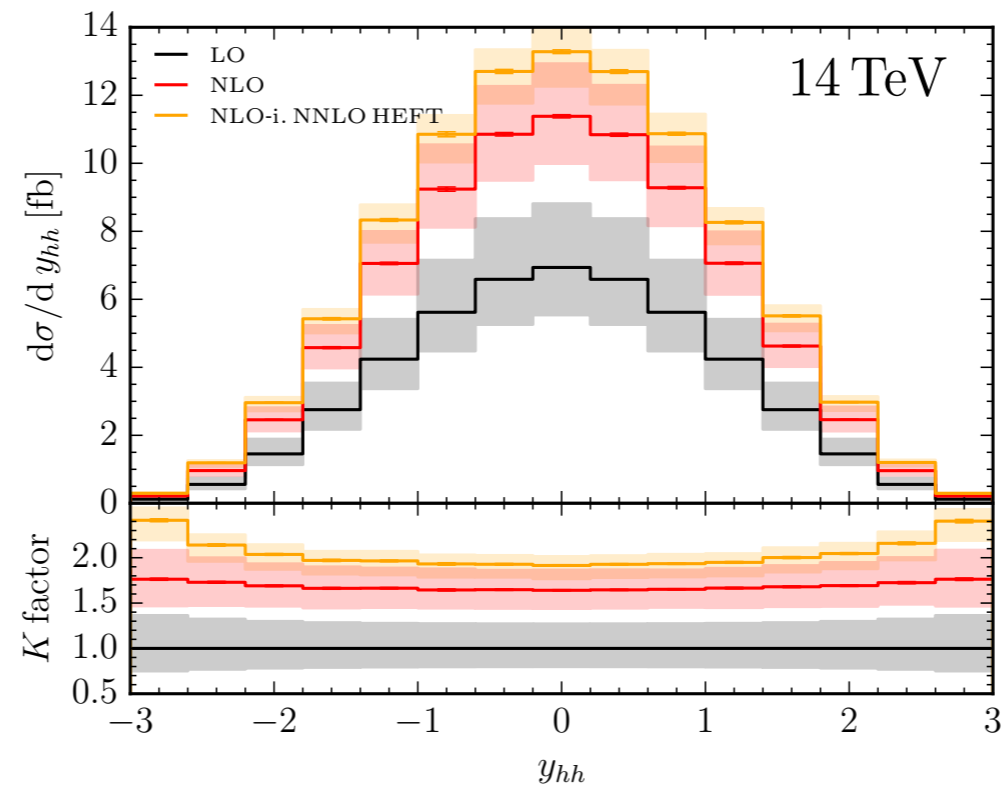
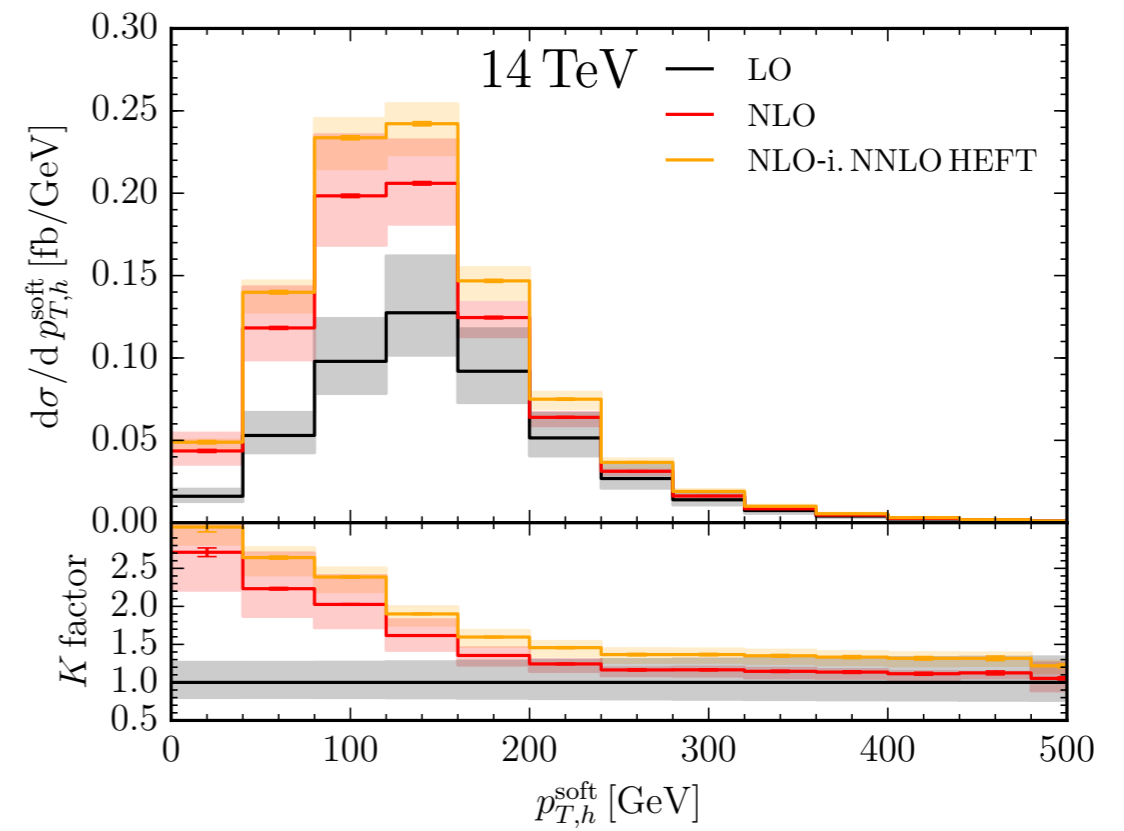
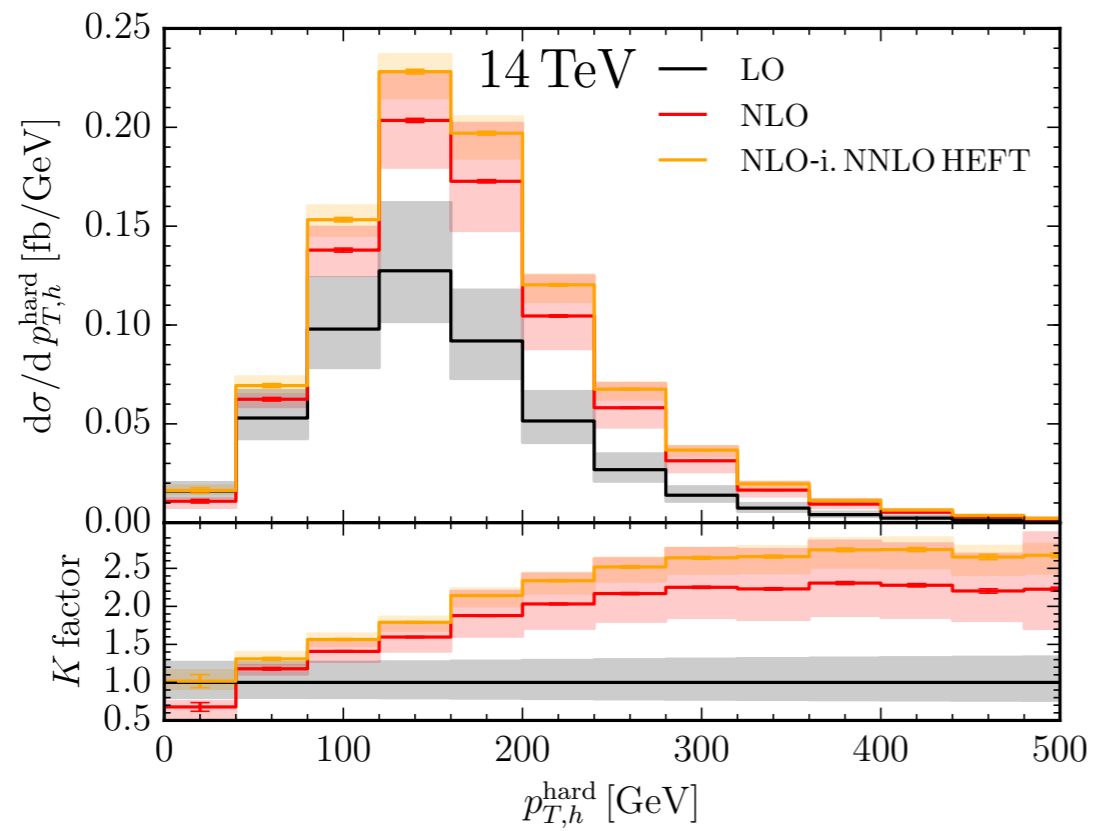
Future

- Fully differential/improved combination with NNLO HEFT
- Grid (faster evaluation of virtuals)
- Parton Shower: POWHEG, MG5_aMC@NLO, Herwig, Sherpa
- EFT/2HDM analysis (?)
- Apply methods/framework GoSam-2L+SecDec to other processes

Thank you for listening!

Backup

NLO Improved NNLO HEFT (II)



Total Cross Section @ 14 TeV

	σ_{LO} (fb)	σ_{NLO} (fb)	σ_{NNLO} (fb)
HEFT	17.07 ^{+30.9%} _{-22.2%}	31.93 ^{+17.6%} _{-15.2%}	37.52 ^{+5.2%} _{-7.6%}
B.I. HEFT	19.85 ^{+27.6%} _{-20.5%}	38.32 ^{+18.1%} _{-14.9%}	43.63 ^{+5.2%*} _{-7.6%}
FTapprox	19.85 ^{+27.6%} _{-20.5%}	34.26 ^{+14.7%} _{-13.2%}	—
Full Theory	19.85 ^{+27.6%} _{-20.5%}	32.91 ^{+13.6%} _{-12.6%}	—
N.I. HEFT	—	32.91 ^{+13.6%} _{-12.6%}	38.67 ^{+5.2%*} _{-7.6%}

PDF4LHC15_nlo_30_pdfas

$m_H = 125$ GeV

$m_T = 173$ GeV

Uncertainty:

$$\mu_R = \mu_F = \frac{m_{HH}}{2}$$

$$\mu \in \left[\frac{\mu_0}{2}, 2\mu_0 \right] \quad (7\text{-point})$$

* re-weighted on total cross-section level

de Florian, Grazzini, Hanga, Kallweit, Lindert, Maierhöfer, Mazzitelli, Rathlev 16;

Maltoni, Vryonidou, Zaro 14 (recalculated by us); Borowka, Greiner, Heinrich, Kerner, Schlenk, Schubert, Zirke 16;

Dawson, Dittmaier, Spira 98 (recalculated by us); Glover, van der Bij 88 (recalculated by us)

Comparison to Full Theory

	$\Delta\sigma_{\text{LO}}^{\text{Full}}$	$\Delta\sigma_{\text{NLO}}^{\text{Full}}$
HEFT	-14%	-3.0%
B.I. HEFT	0%	+16%
FTapprox	0%	+4.1%

Can do a similar exercise @ 100 TeV, differences typically larger

YR4 Numbers

YR4 Prescription:

$$\sigma(gg \rightarrow hh)_{NLO}^{exact} = \sigma(gg \rightarrow hh)_{NLO}^{HEFT} (1 + \delta_t)$$

$$\sigma'_{NNLL} = \sigma_{NNLL} + \delta_t \sigma_{NLO}^{HEFT}$$

\sqrt{s}	σ'_{NNLL} (fb)	Scale Unc. (%)	PDF Unc. (%)	α_S Unc. (%)
7 TeV	7.078	+4.0 – 5.7	± 3.4	± 2.8
8 TeV	10.16	+4.1 – 5.7	± 3.1	± 2.6
13 TeV	33.53	+4.3 – 6.0	± 2.1	± 2.3
14 TeV	39.64	+4.4 – 6.0	± 2.1	± 2.2

Checks

Real Emission & Catani-Seymour Subtraction Terms Catani, Seymour 96

Independence of dipole cut parameter Nagy 03

Real + HEFT agrees with MG5_AMC@NLO

Maltoni, Vryonidou, Zaro 14

Virtual Corrections

2 calculations of unreduced amplitude

2 calculations of mass renormalization (CT vs $d\mathcal{M}^{\text{LO}}/dm_T^2$ numerically)

(Some) integrals cross-checked with VEGAS Lepage 80; Hahn (Cuba)

Amplitude invariant under crossing

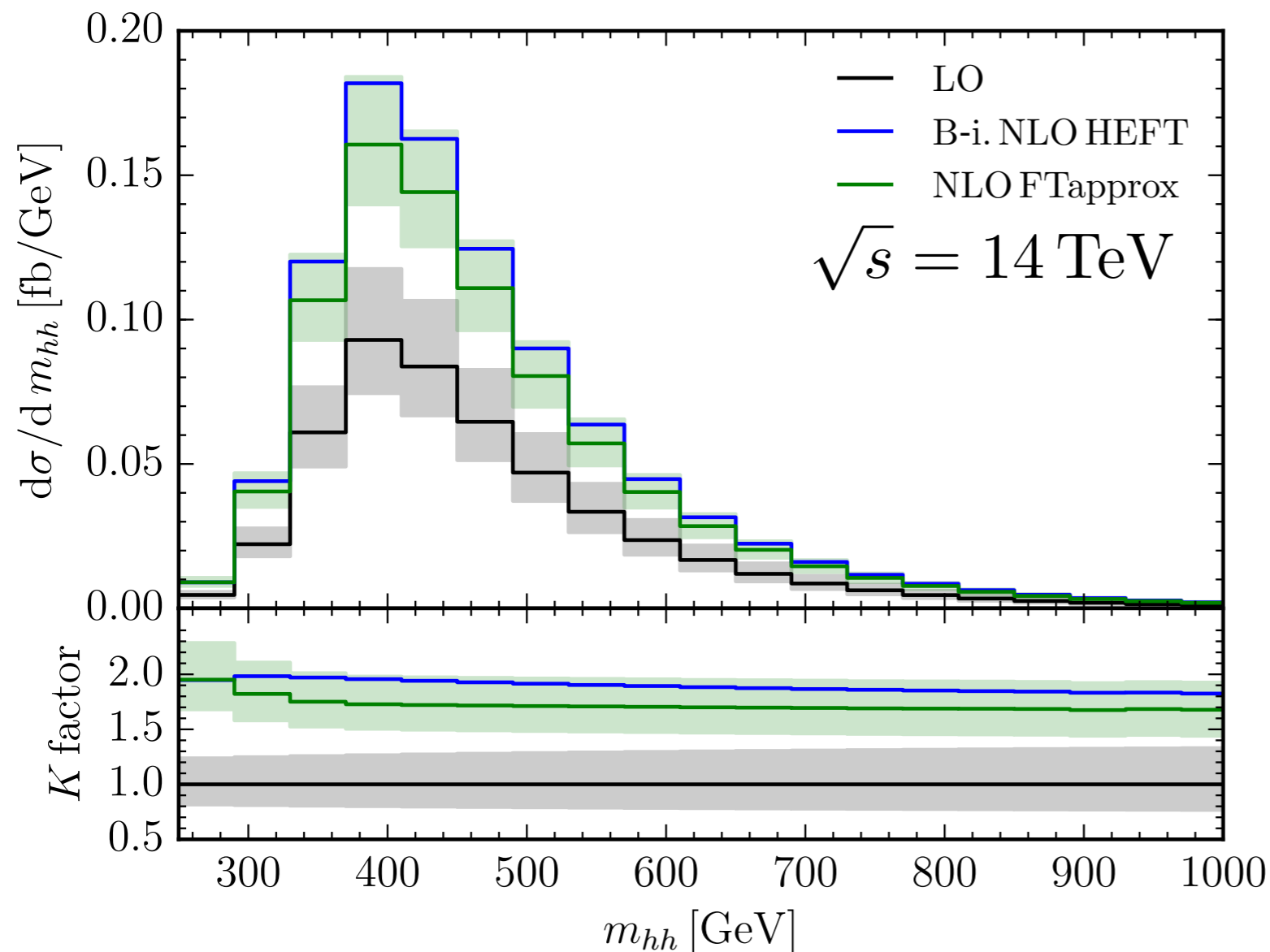
Numerical pole cancellation (5 digits)

Single Higgs production part agrees with **SusHi** Harlander, Liebler, Mantler 13,16;

$1/m_T$ result converges to full result below top threshold

Grigo, Hoff, Steinhauser 15

A. FT approx

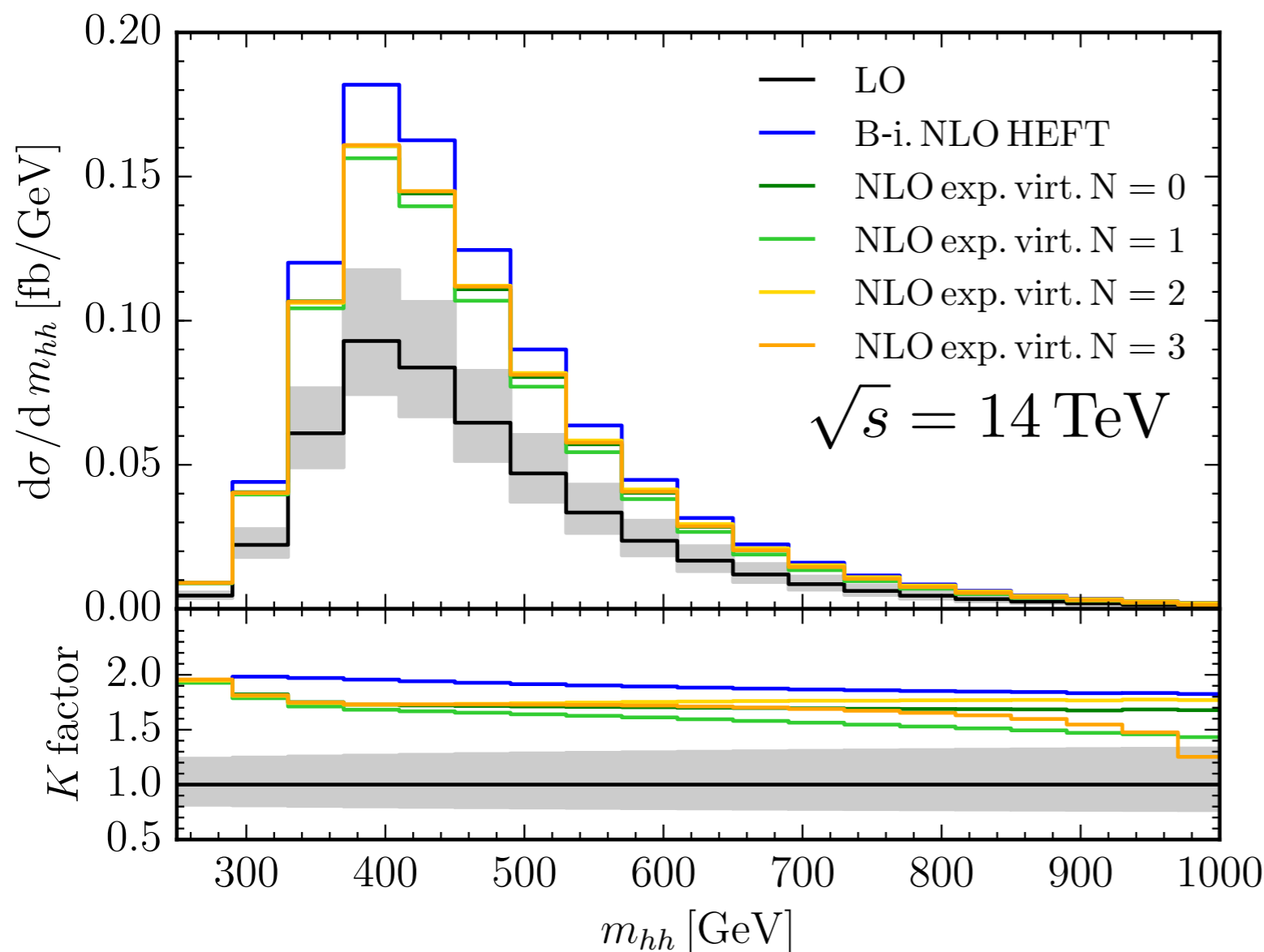


Distribution: Agreement between HEFT approximations in first bin where $\sqrt{\hat{s}} \approx 2m_H$, not much hard real emission

Total: m_T in only reals suppresses XS by 11% compared to HEFT

	σ_{LO} (fb)	σ_{NLO} (fb)
B.I. HEFT	$19.85^{+27.6\%}_{-20.5\%}$	$38.32^{+18.1\%}_{-14.9\%}$
FTapprox	$19.85^{+27.6\%}_{-20.5\%}$	$34.26^{+14.7\%}_{-13.2\%}$
Full Theory	$19.85^{+27.6\%}_{-20.5\%}$...

B. Expansion in Top Quark Mass



Low m_{hh} : Expansion seems ok in first bin

$$\sqrt{\hat{s}} < 2m_T$$

Increasing m_{hh} : Fewer reasons to trust expansion

Total: $\mathcal{O}(5\%)$ differences between first few terms of expansion

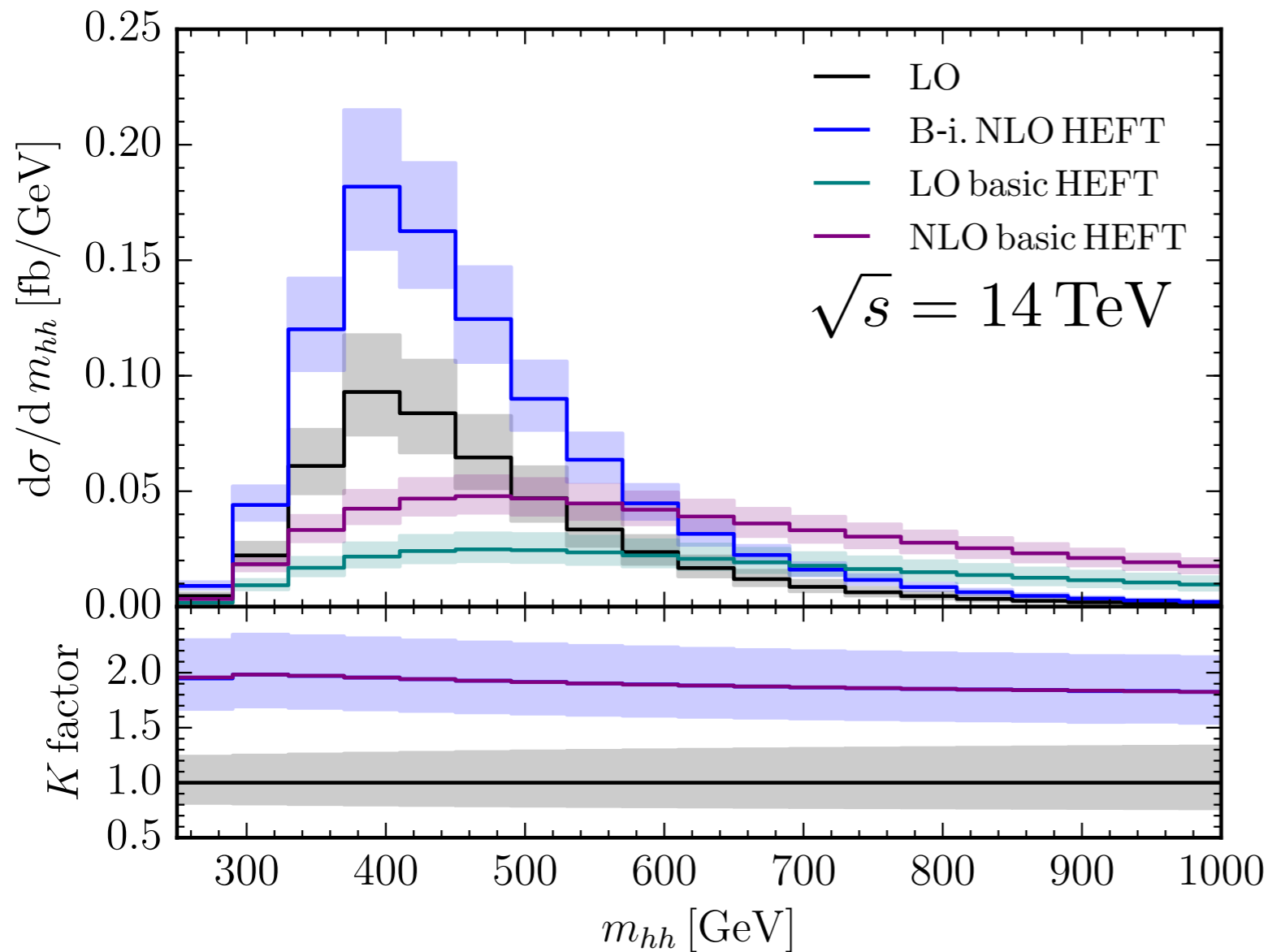
(Tom Zirke) Virtuals: asymptotic expansion in $1/m_T^2$ (q2e/exp+ Reduze + matad)

Harlander, Seidensticker, Steinhauser 97,99; von Manteuffel, Studerus 12; Steinhauser 00

Mass effects give large uncertainty

Required NLO calculation with full mass dependence

LO & Born Improved NLO HEFT



PDF4LHC15_nlo_30_pdfas

$m_H = 125 \text{ GeV}$

$m_T = 173 \text{ GeV}$

Uncertainty:

$$\mu_R = \mu_F = \frac{m_{HH}}{2}$$

$$\mu \in \left[\frac{\mu_0}{2}, 2\mu_0 \right] \quad (7\text{-point})$$

LO: HEFT describes distributions poorly, underestimates

XS @ LO by 14%

NLO: HEFT indicates

$$K \approx 2$$

	σ_{LO} (fb)	σ_{NLO} (fb)
HEFT	$17.07^{+30.9\%}_{-22.2\%}$	$31.93^{+17.6\%}_{-15.2\%}$
B.I. HEFT	$19.85^{+27.6\%}_{-20.5\%}$	$38.32^{+18.1\%}_{-14.9\%}$
Full Theory	$19.85^{+27.6\%}_{-20.5\%}$...

NLO HEFT

Born Improved NLO QCD HEFT

$$d\sigma_{\text{NLO}}(m_T) \approx d\bar{\sigma}_{\text{NLO}}(m_T) \equiv \frac{d\sigma_{\text{NLO}}(m_T \rightarrow \infty)}{d\sigma_{\text{LO}}(m_T \rightarrow \infty)} d\sigma_{\text{LO}}(m_T)$$

$$K \approx 2$$

A. FTapprox

Maltoni et al.14

$$d\bar{\sigma}^V(m_T)$$

$$d\sigma^R(m_T)$$

−10%

B. Expansion

Grigo, Hoff, Steinhauser 15

$$d\hat{\sigma}(m_T) \equiv d\sigma_0 + d\sigma_1 \frac{m_H^2}{m_T^2} + \dots + d\sigma_6 \frac{m_H^{12}}{m_T^{12}}$$

$$d\bar{\sigma}_{\text{NLO}}^{SV}(m_T) \equiv d\hat{\sigma}_{\text{NLO}}^{SV}(m_T) \frac{d\sigma_{\text{LO}}^V(m_T)}{d\hat{\sigma}_{\text{LO}}^V(m_T)}$$

$$d\bar{\sigma}_{\text{NLO}}^H(m_T) \equiv d\hat{\sigma}_{\text{NLO}}^H(m_T) \frac{\sigma_{\text{LO}}^V(m_T)}{\hat{\sigma}_{\text{LO}}^V(m_T)}$$

±10%

Top-quark Width Effects

Total XS @ LO: reduced by 2% by including top-quark width

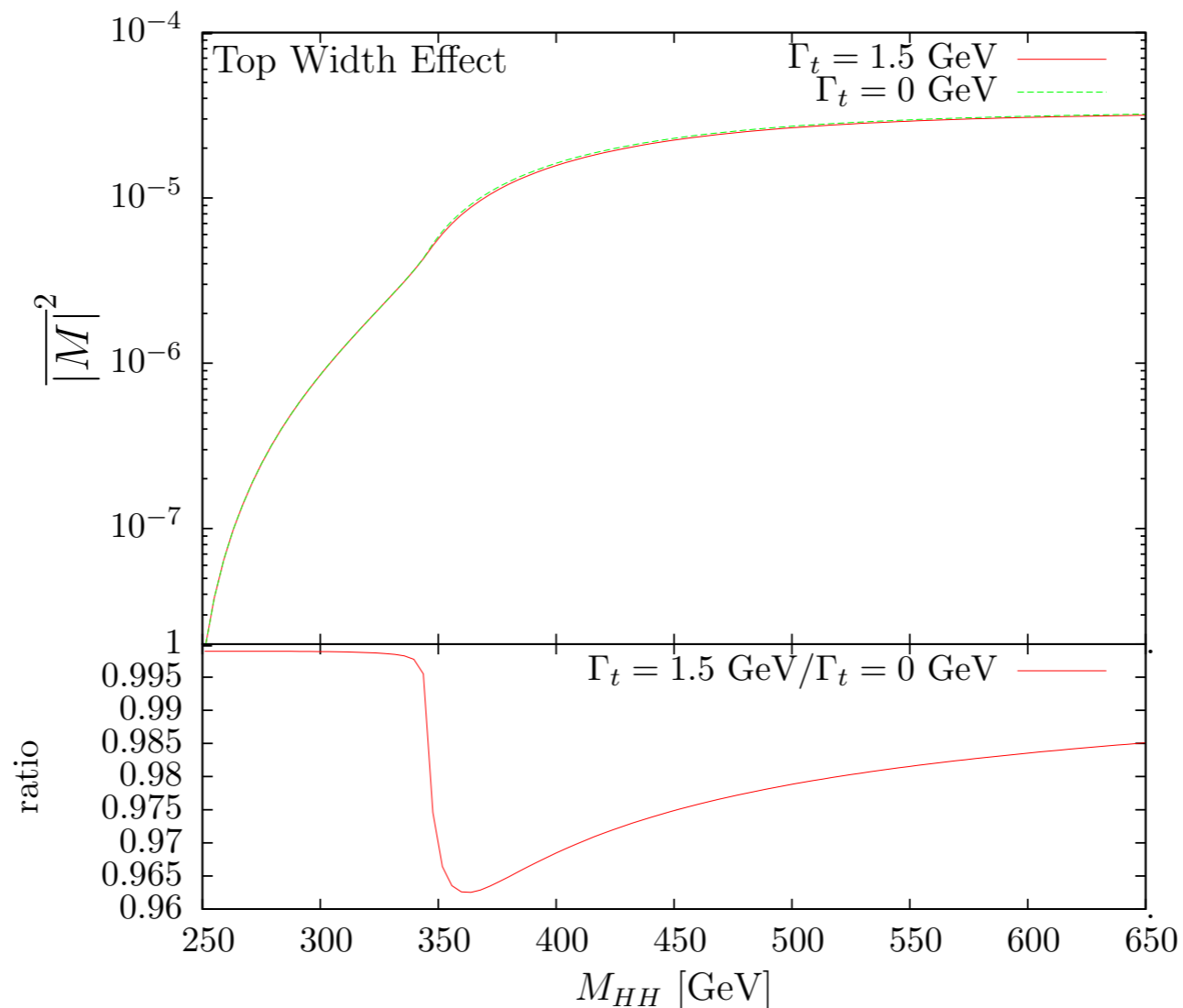
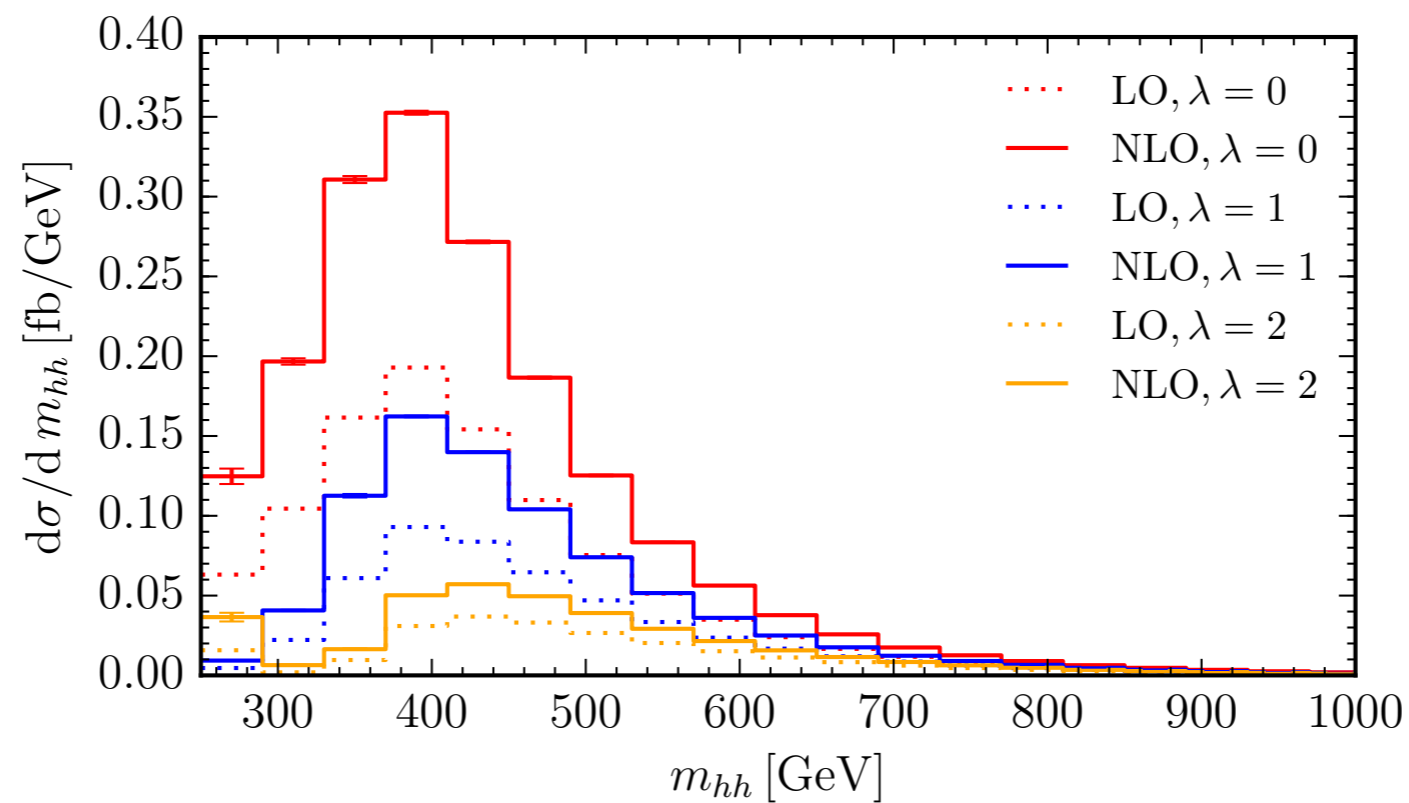
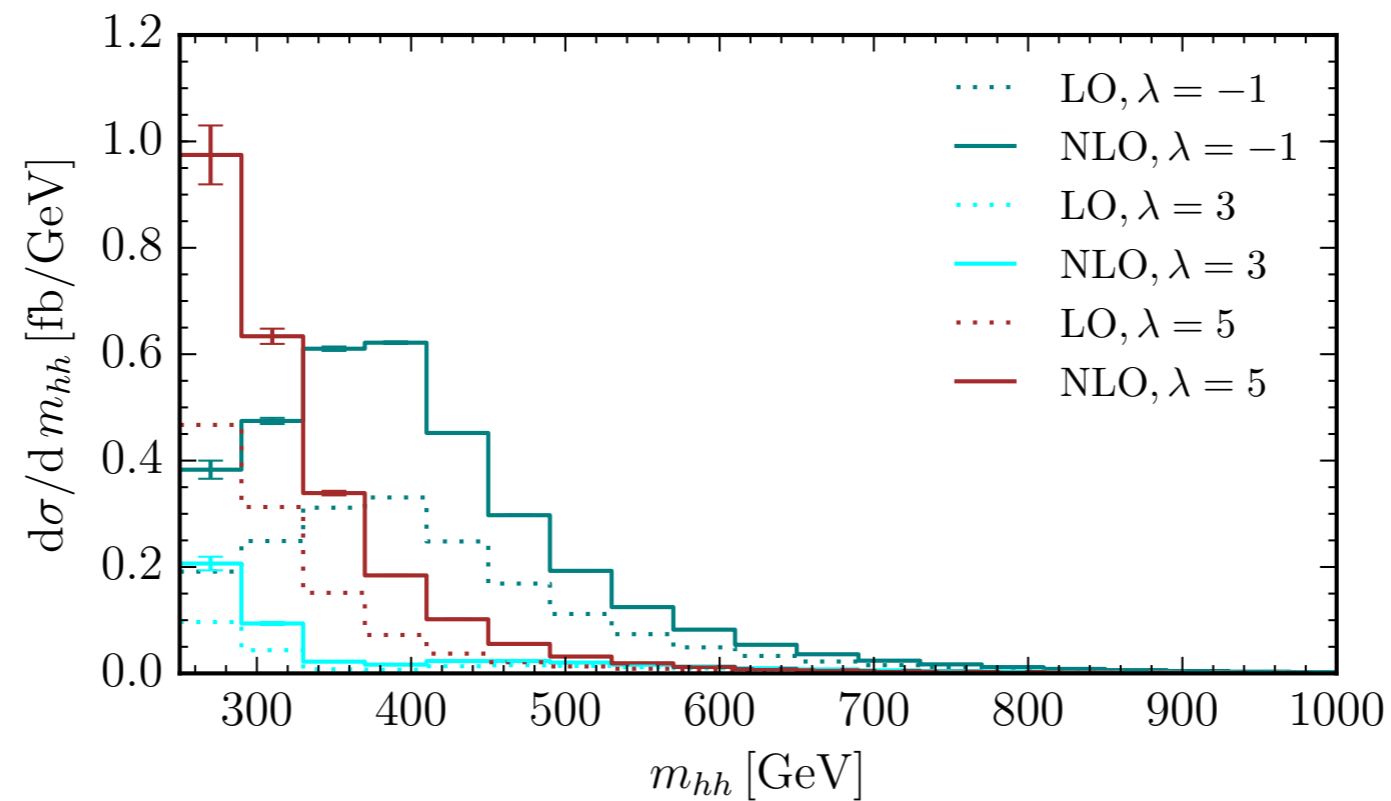


Figure 3: Top width effect on the one-loop (Born) matrix element squared for $gg \rightarrow HH$. The results for $\Gamma_t = 0$ and 1.5 GeV are shown along with the corresponding ratio.

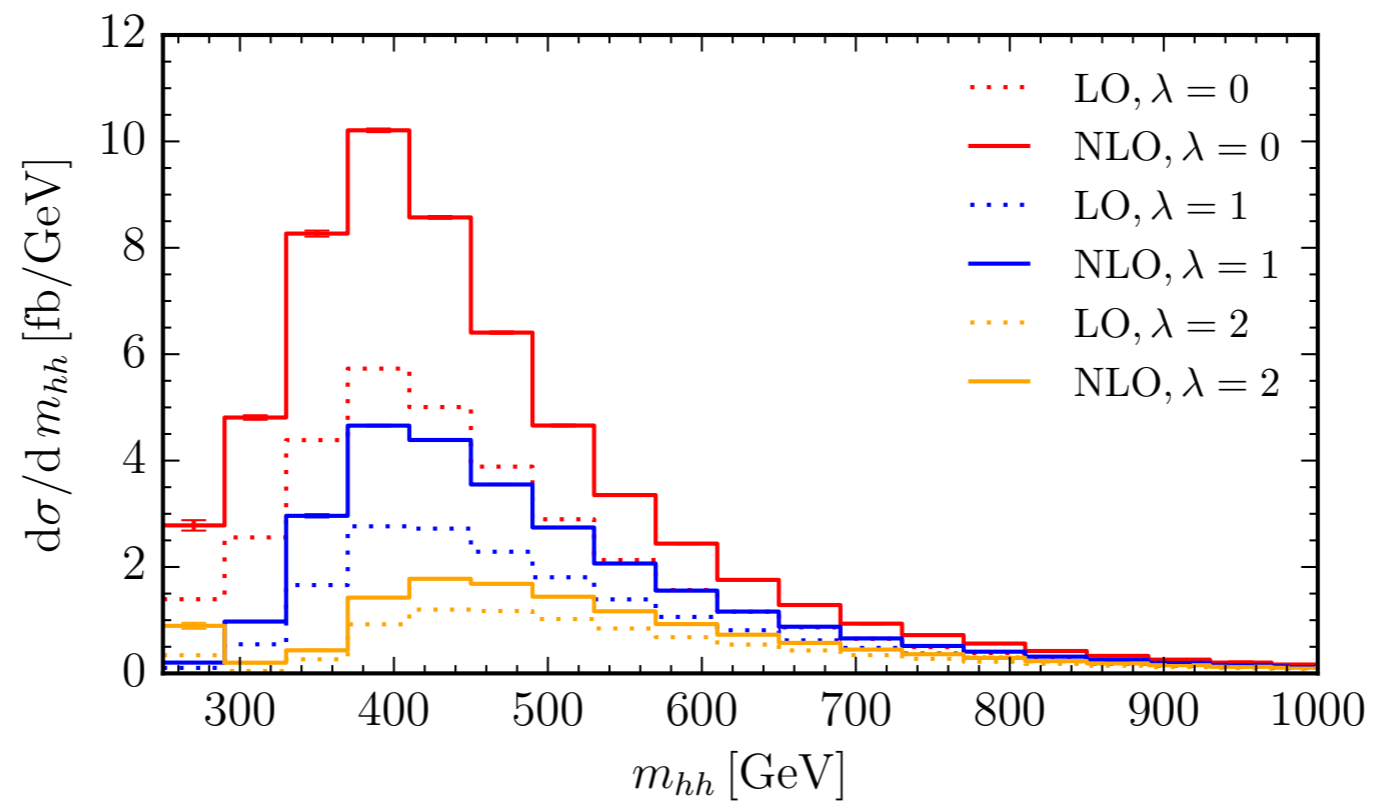
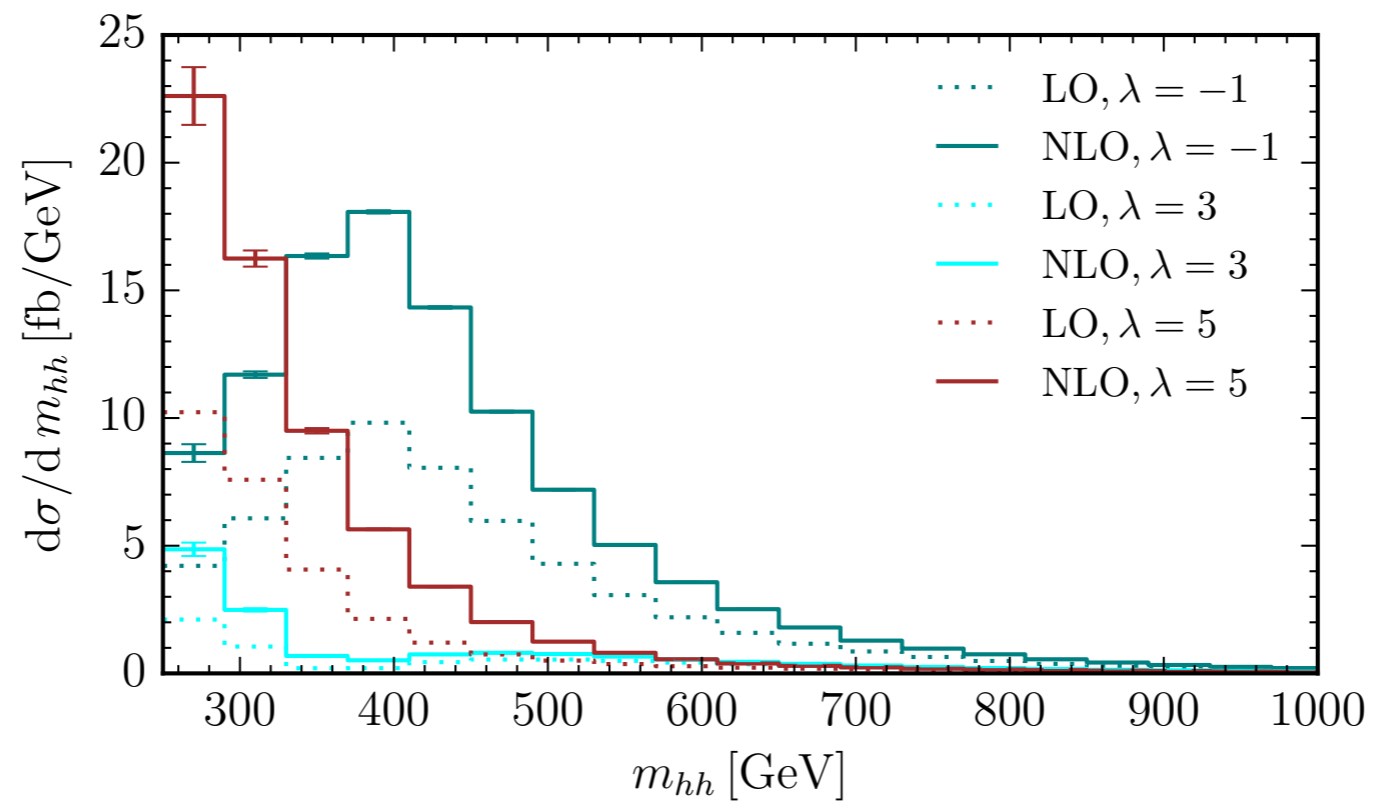
Lambda Variation

$\sqrt{s} = 14 \text{ TeV}$



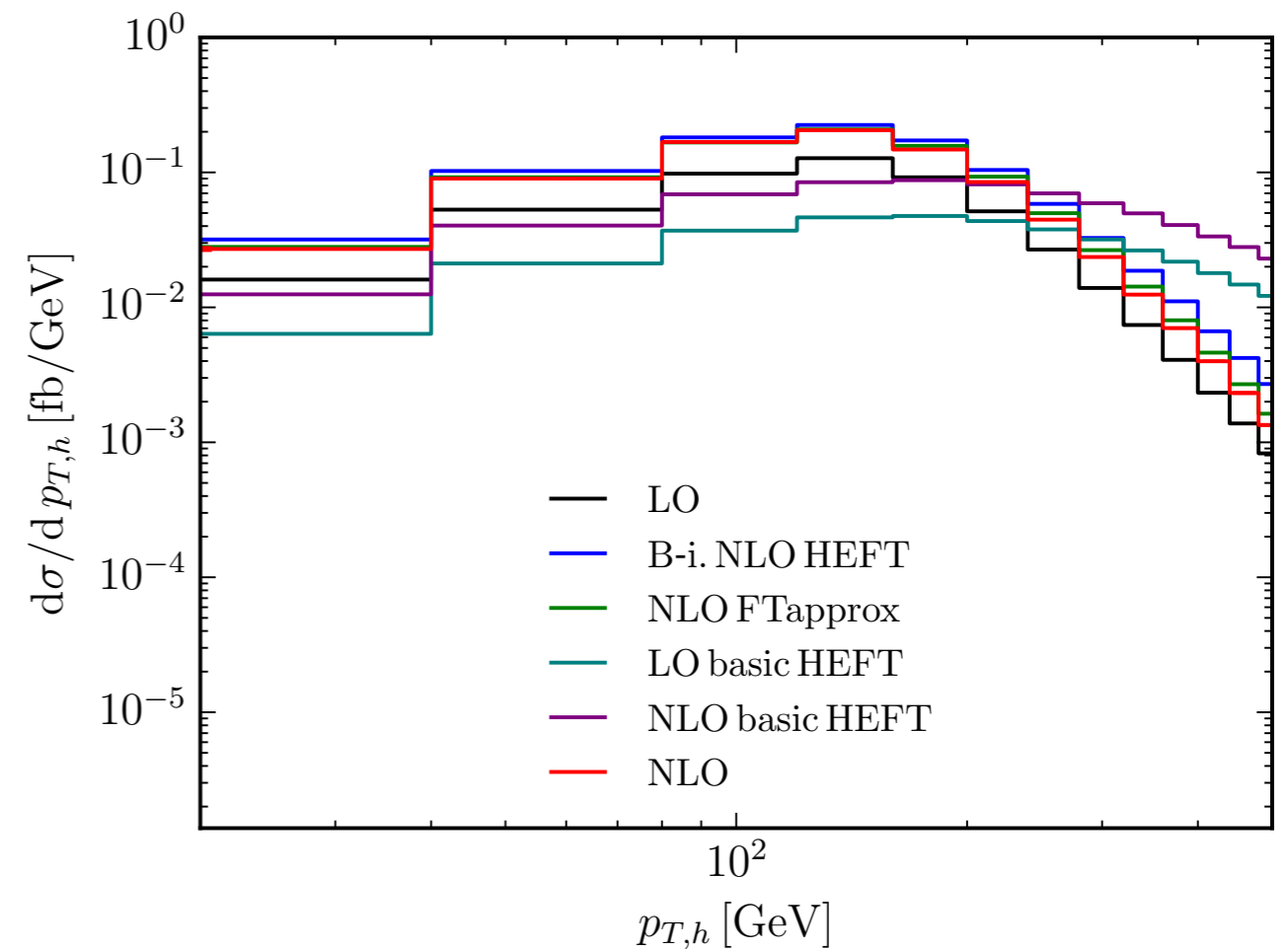
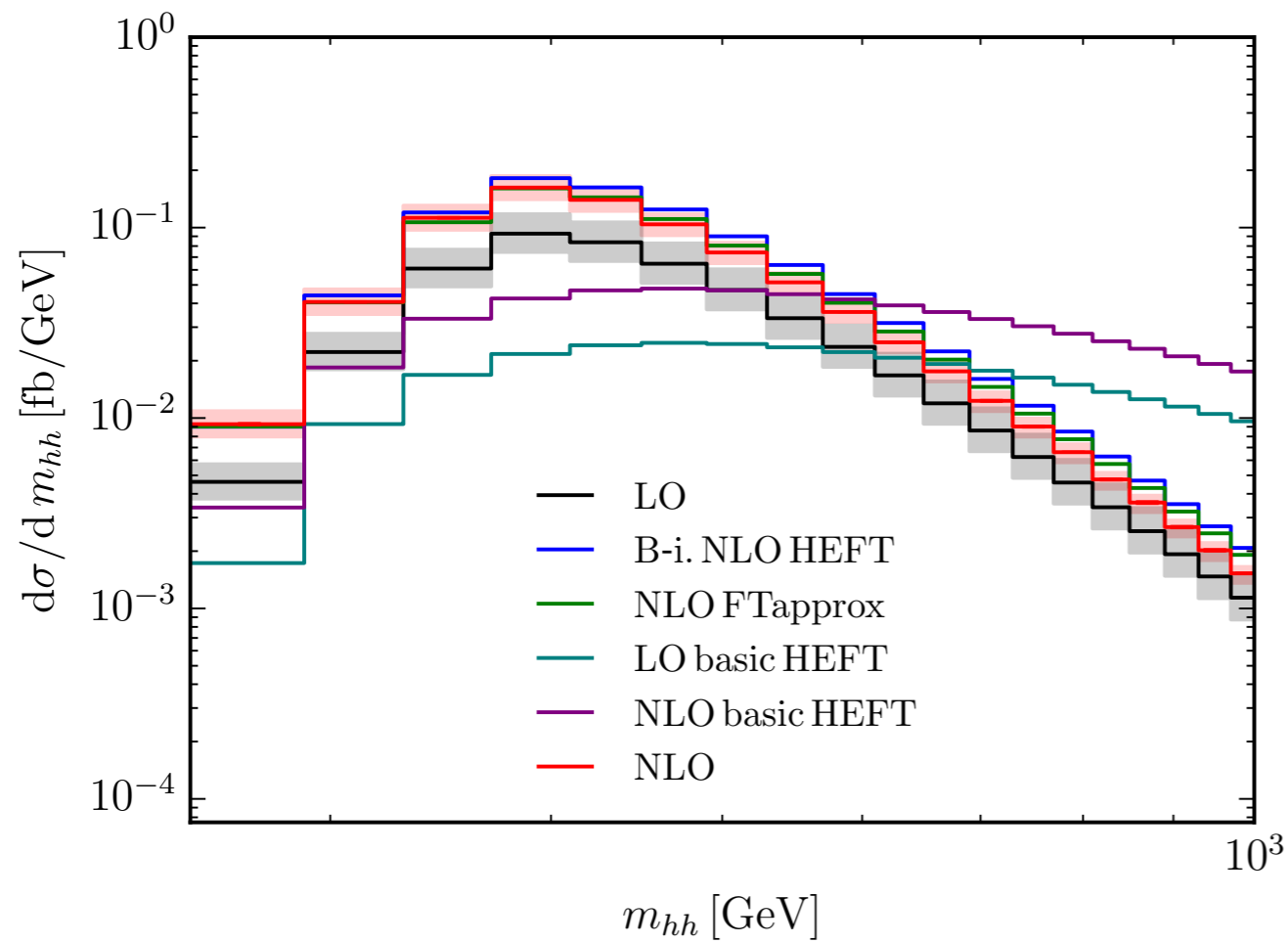
Lambda Variation

$\sqrt{s} = 100 \text{ TeV}$



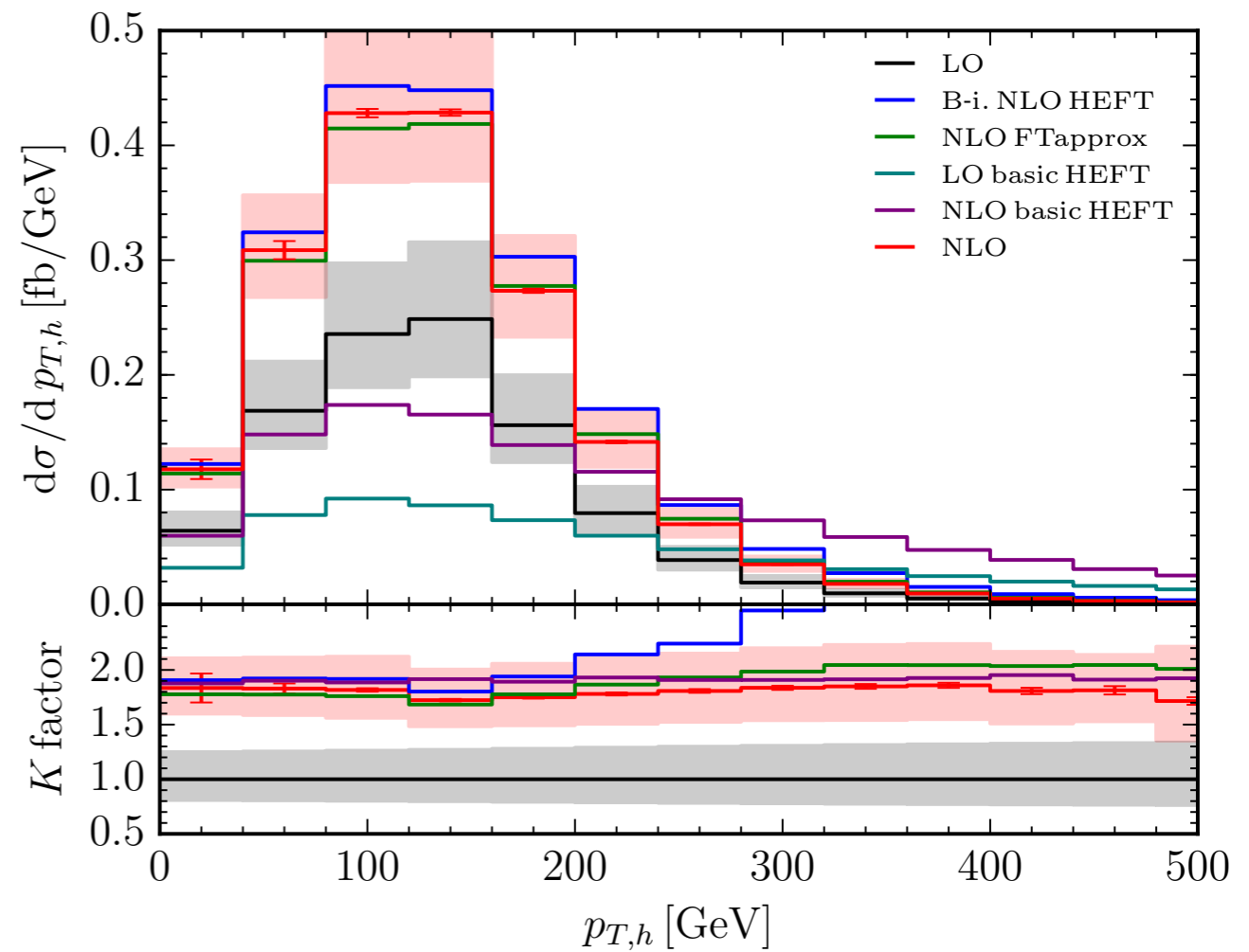
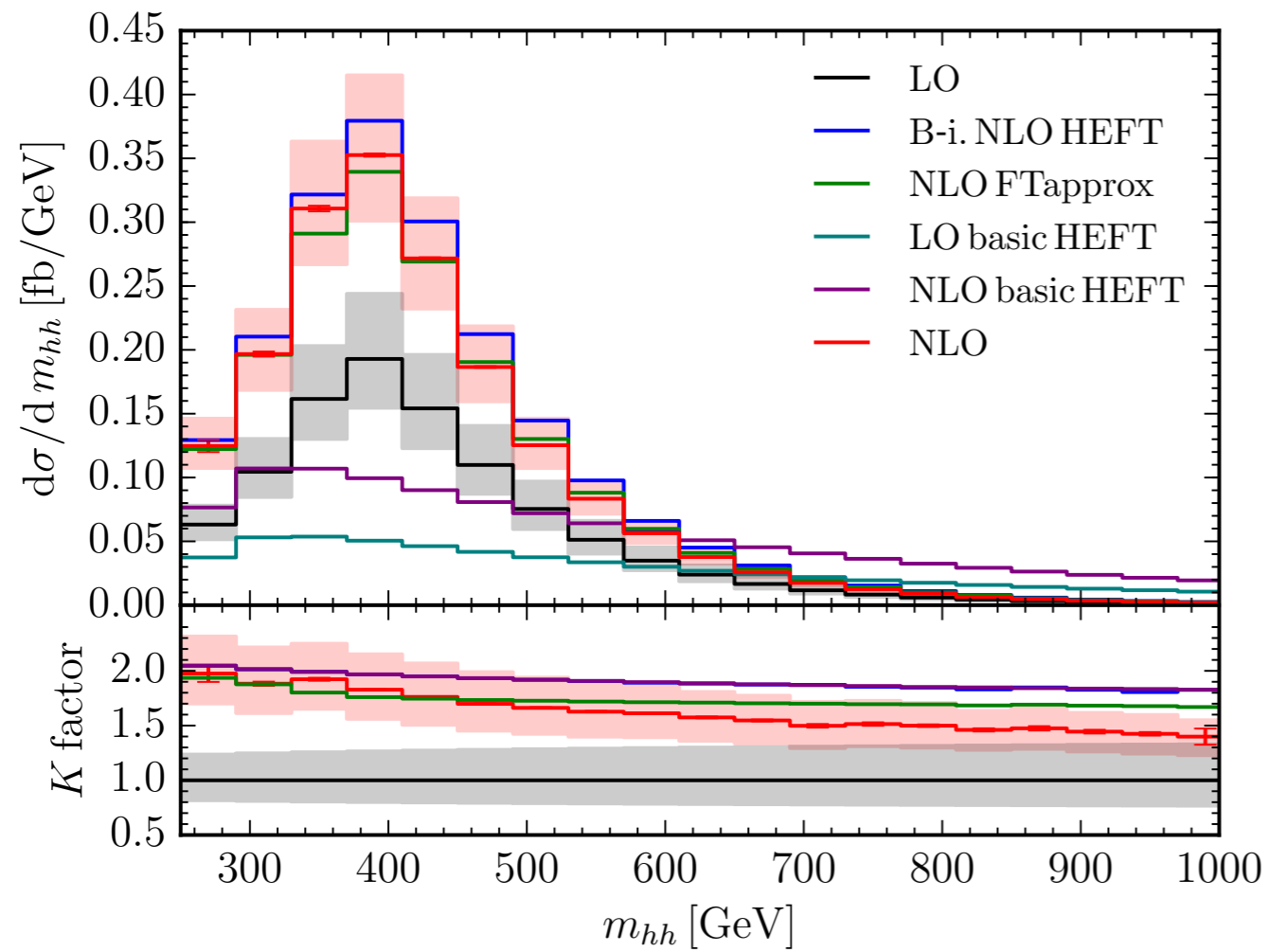
Scaling

$\sqrt{s} = 14 \text{ TeV}$



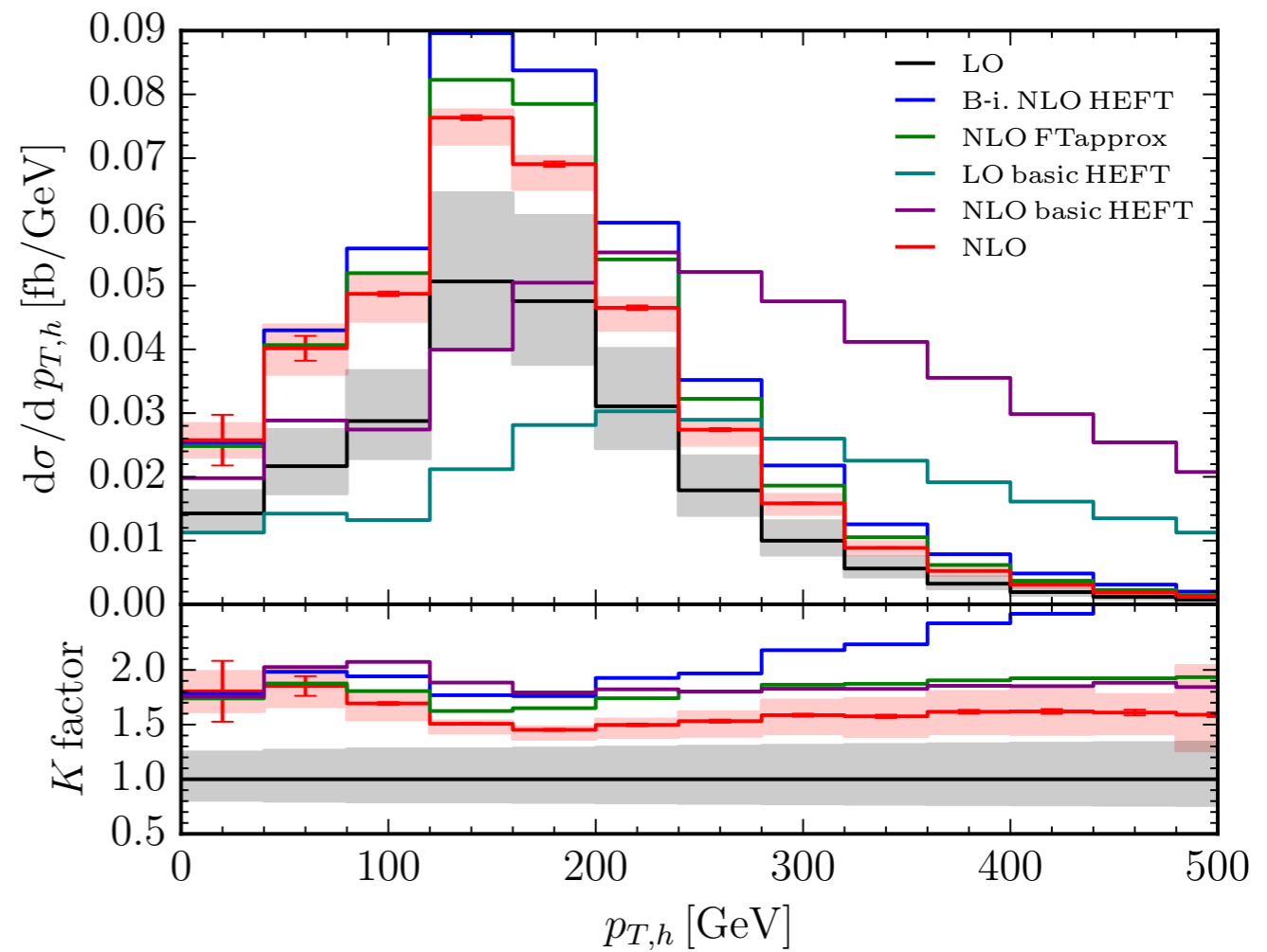
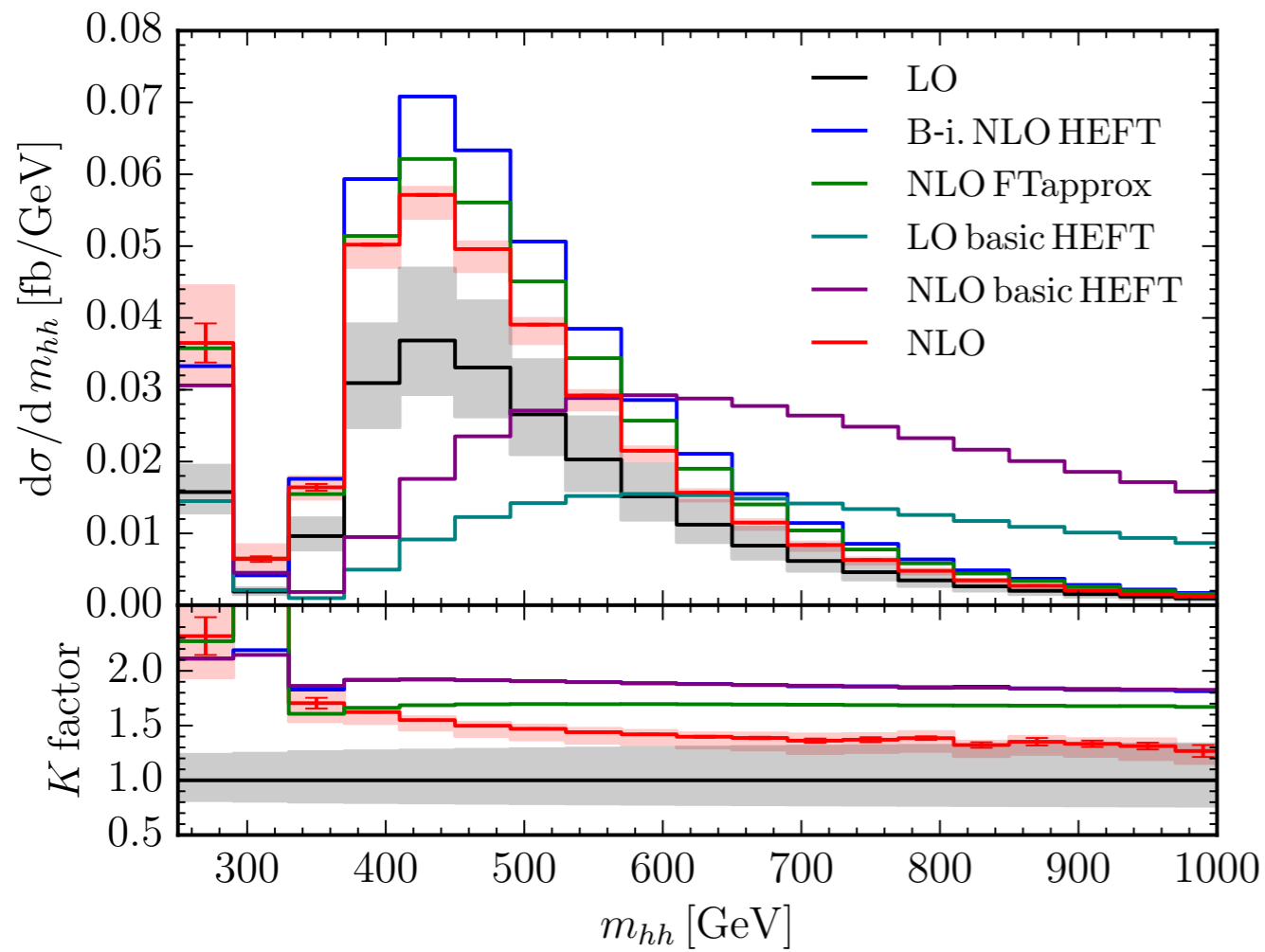
Lambda 0 x SM

$\sqrt{s} = 14 \text{ TeV}$



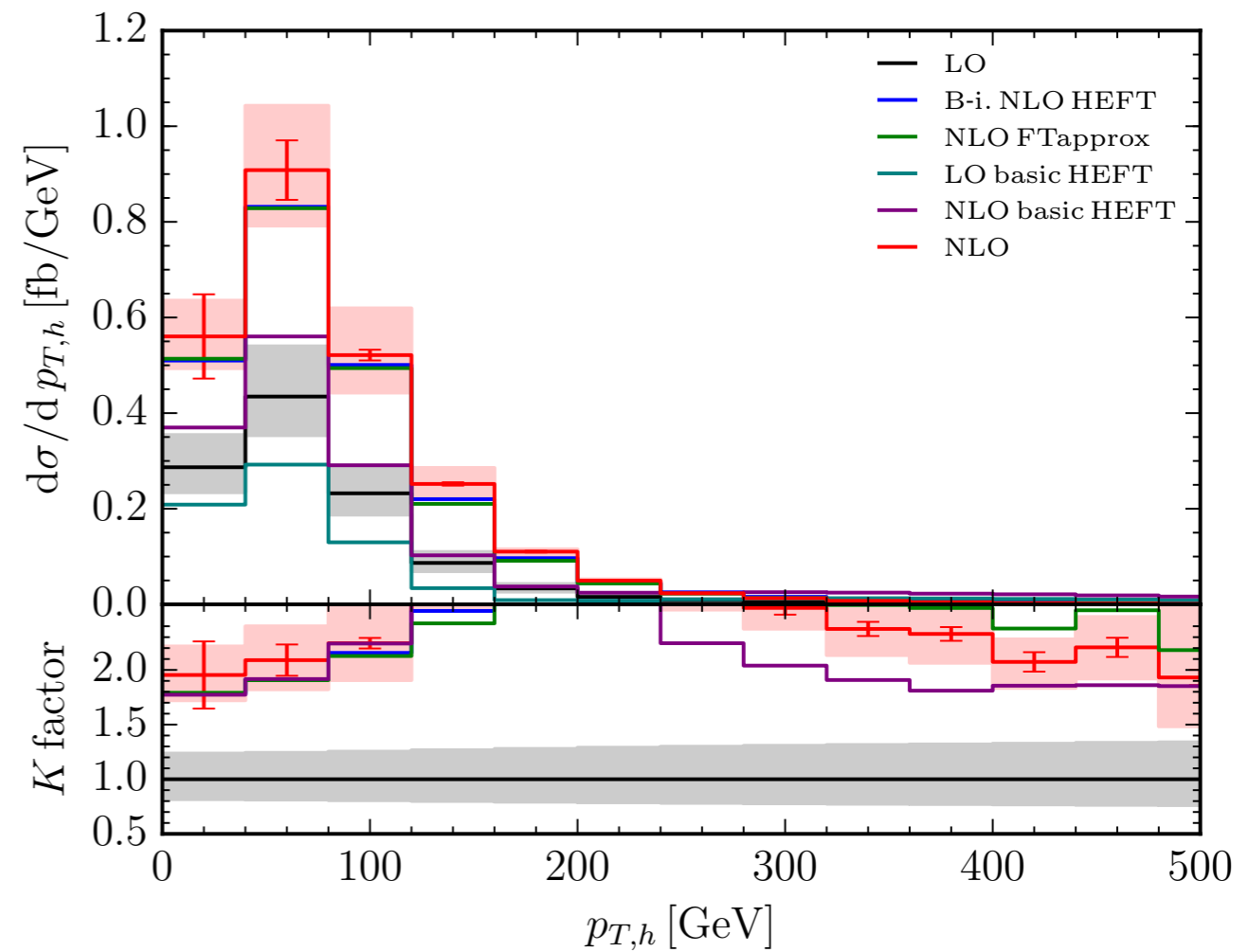
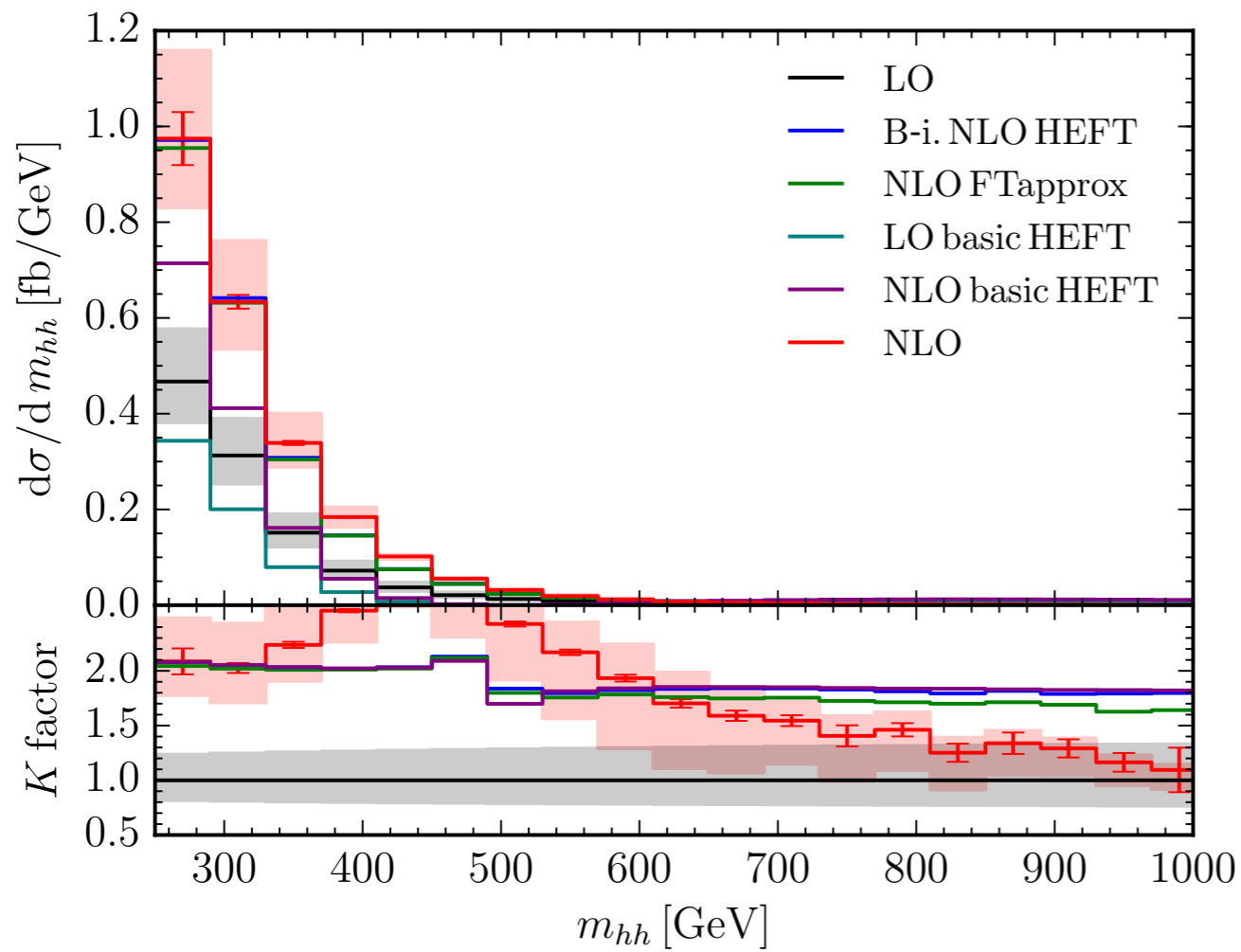
Lambda 2 x SM

$\sqrt{s} = 14 \text{ TeV}$



Lambda 5 x SM

$\sqrt{s} = 14 \text{ TeV}$



Amplitude Structure

$\overline{\text{MS}}$ scheme strong coupling a and OS top-quark mass:

$$F = aF^{(1)} + a^2(\delta Z_A + \delta Z_a)F^{(1)} + a^2\delta m_t^2 F^{ct,(1)} + a^2F^{(2)} + O(a^3)$$

$$F^{(1)} = \left(\frac{\mu_R^2}{M^2}\right)^\epsilon \left[b_0^{(1)} + b_1^{(1)}\epsilon + b_2^{(1)}\epsilon^2 + \mathcal{O}(\epsilon^3) \right] \longleftarrow \text{1-loop}$$

$$F^{ct,(1)} = \left(\frac{\mu_R^2}{M^2}\right)^\epsilon \left[c_0^{(1)} + c_1^{(1)}\epsilon + \mathcal{O}(\epsilon^2) \right] \longleftarrow \text{Mass Counter-Terms}$$

$$F^{(2)} = \left(\frac{\mu_R^2}{M^2}\right)^{2\epsilon} \left[\frac{b_{-2}^{(2)}}{\epsilon^2} + \frac{b_{-1}^{(2)}}{\epsilon} + b_0^{(2)} + \mathcal{O}(\epsilon) \right] \longleftarrow \text{2-loop}$$

Red terms contain integrals, computed numerically at each PS point, not re-evaluated for scale variations

Real Radiation (HH + j...):

$$gg \rightarrow HH + g \quad g\bar{q} \rightarrow HH + \bar{q}$$

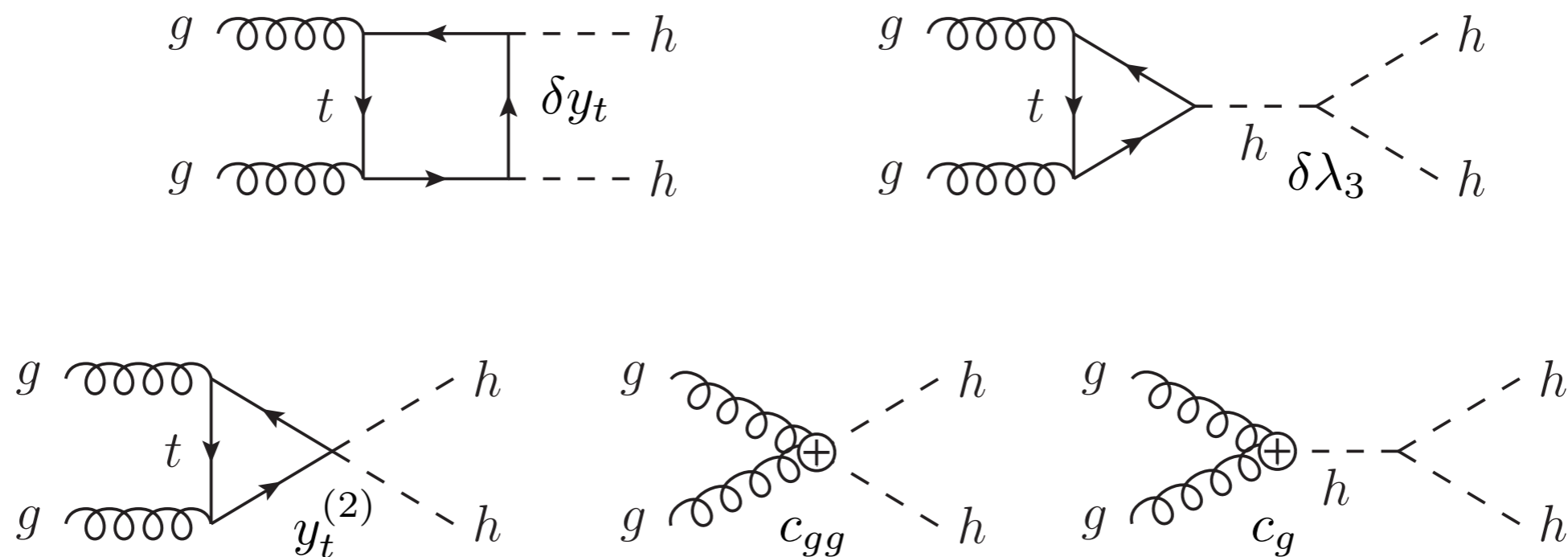
$$q\bar{q} \rightarrow HH + g \quad gq \rightarrow HH + q$$

GoSam for MEs [Cullen et al. 14](#)

Catani-Seymour Dipole Subtraction [Catani, Seymour 96](#)

BSM EFT

Parametrise **non-resonant** new physics with EFT (5 parameters):



Azatov, Contino, Panico, Son 15;

(Cluster analysis) Dall'Osso, Dorigo, Gottardo, Oliveira, Tosi, Goertz 15;

+ Carvalho, Manzano, Dorigo, Gouzevich 16;

(B.I. HEFT) Gröber, Mühlleitner, Spira, Streicher 15;

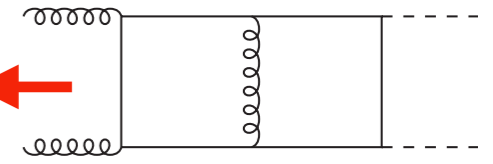
12 representative
"clusters"

Amplitude Evaluation (II)

Contributing integrals:

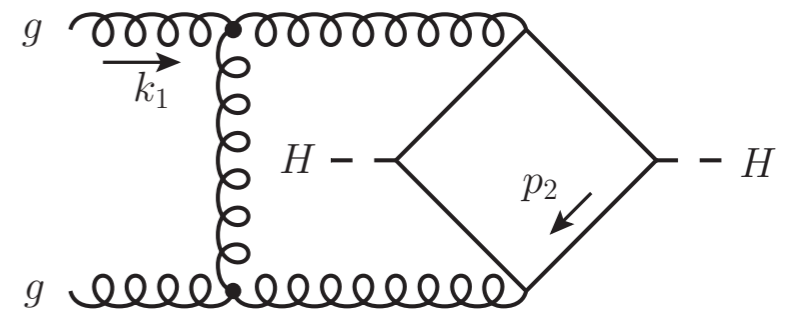
$$\sqrt{s} = 327.25 \text{ GeV}, \quad \sqrt{-t} = 170.05 \text{ GeV}, \quad M^2 = s/4$$

integral	value	error	time [s]
...			
F1_011111110_ord0	(0.484, 4.96e-05)	(4.40e-05, 4.23e-05)	11.8459
...			
N3_111111100_k1p2k2p2_ord0	(0.0929, -0.224)	(6.32e-05, 5.93e-05)	235.412
N3_111111100_1_ord0	(-0.0282, 0.179)	(8.01e-05, 9.18e-05)	265.896
N3_111111100_k1p2k1p2_ord0	(0.0245, 0.0888)	(5.06e-05, 5.31e-05)	282.794
N3_111111100_k1p2_ord0	(-0.00692, -0.108)	(3.05e-05, 3.05e-05)	433.342



$$I(s, t, m_t^2, m_h^2) = - \left(\frac{\mu^2}{M^2} \right)^{2\epsilon} \Gamma(3 + 2\epsilon) M^{-4} \left(\frac{A_{-2}}{\epsilon^2} + \frac{A_{-1}}{\epsilon^1} + A_0 + \mathcal{O}(\epsilon) \right)$$

Sector Decomposition



sector	integral value	error	time [s]	#points
5	(-1.34e-03, 2.00e-07)	(2.38e-07, 2.69e-07)	0.255	1310420
6	(-1.58e-03, -9.23e-05)	(7.44e-07, 5.34e-07)	0.266	1310420
...				
41	(0.179, -0.856)	(1.10e-05, 1.22e-05)	29.484	79952820
42	(0.359, -1.308)	(1.40e-06, 1.58e-06)	80.24	211436900
44	(0.0752, -1.185)	(5.44e-07, 6.76e-07)	99.301	282904860

Slide:
Matthias Kerner
(LL 2016)

Rank 1 Shifted Lattices

$\mathcal{O}(n^{-1})$ algorithm for numerical integration:

Review: Dick, Kuo, Sloan 13

$$I_s[f] \equiv \int_{[0,1]^s} d^s x f(\vec{x})$$

$$f : \mathbb{R}^s \rightarrow \mathbb{C}$$

$$I_s[f] \approx \bar{Q}_{s,n,m}[f] \equiv \frac{1}{m} \sum_{k=1}^m \frac{1}{n} \sum_{i=0}^{n-1} f \left(\left\{ \frac{i\vec{z}}{n} + \vec{\Delta}_k \right\} \right)$$

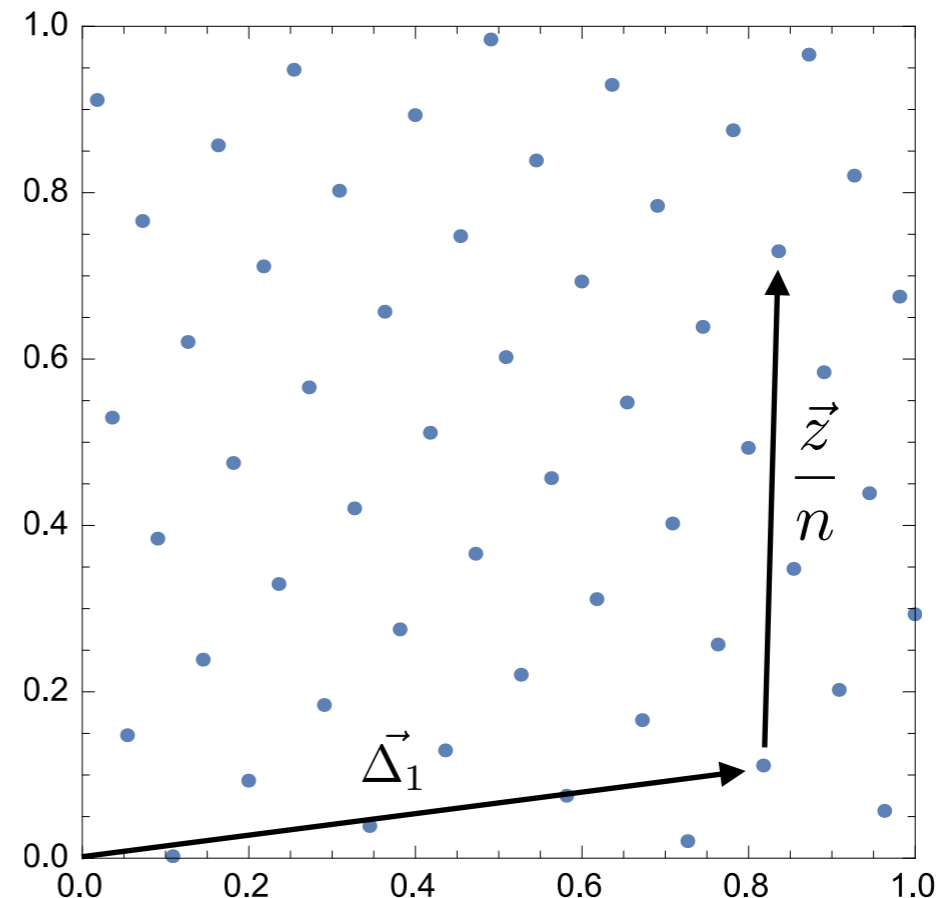
\vec{z} - Generating vec.

$\vec{\Delta}_k$ - Random shift vec.

$\{ \}$ - Fractional part

n - # Lattice points

m - # Random shifts

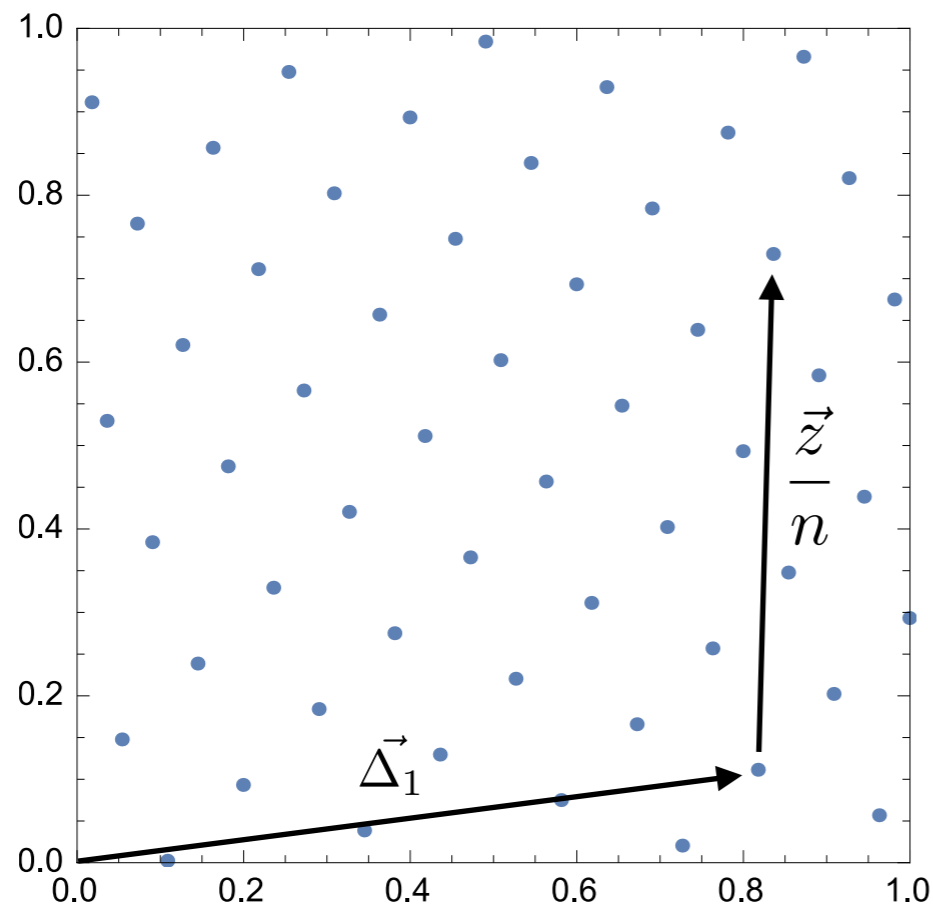


Generating vector \vec{z} precomputed for a **fixed** number of lattice points, chosen to minimise worst-case error [Nuyens 07](#)

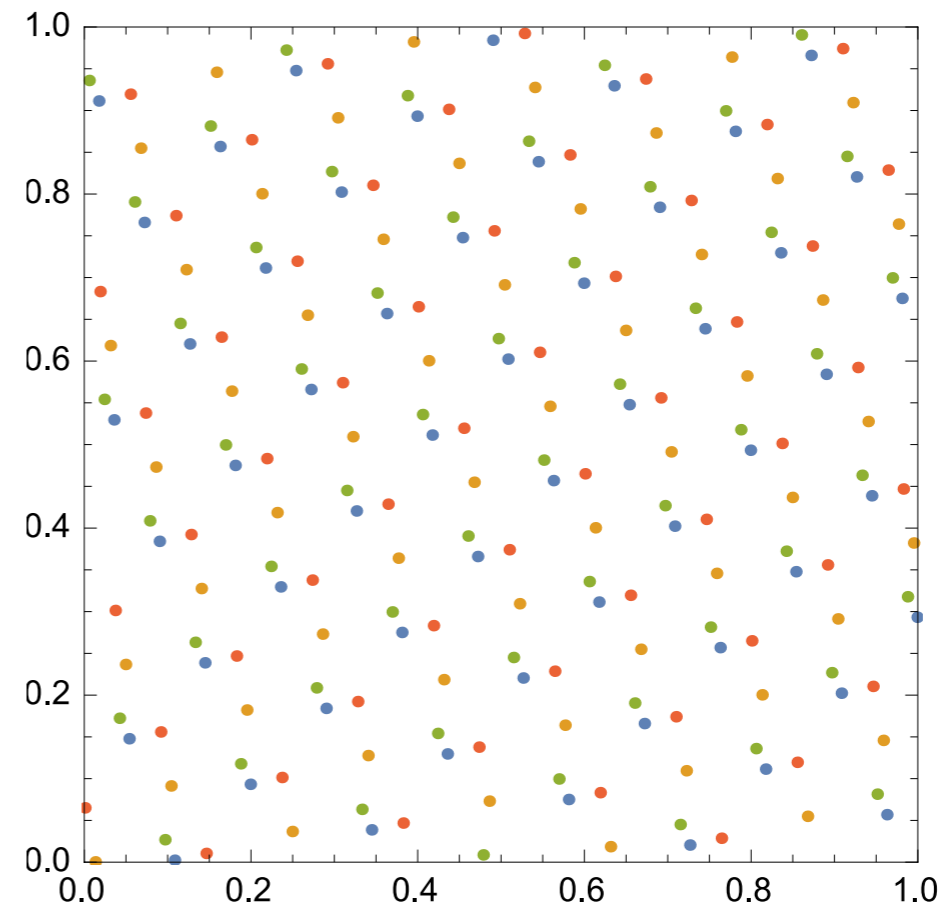
Rank 1 Shifted Lattices (II)

Unbiased error estimate computed from random shifts:

$$\text{Var}[\bar{Q}_{s,n,m}[f]] \approx \frac{1}{m(m-1)} \sum_{k=1}^m (Q_{s,n,k} - \bar{Q}_{s,n,m})^2$$



1 Shift

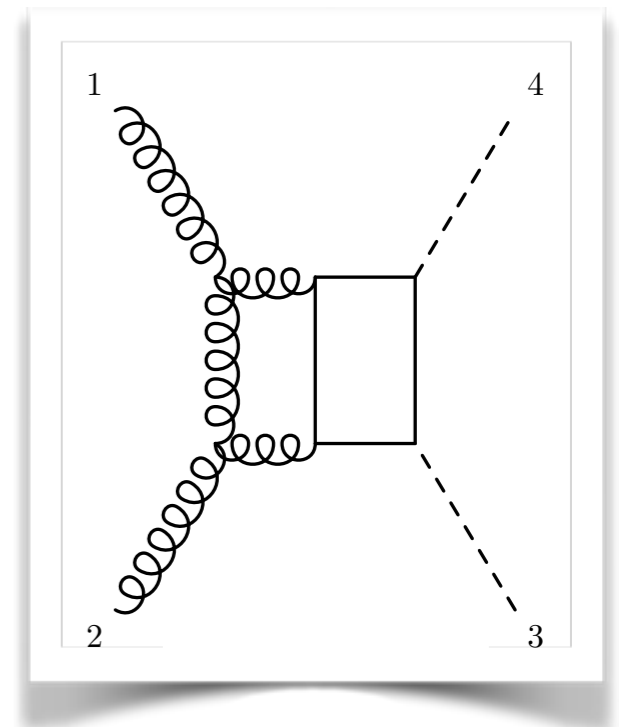
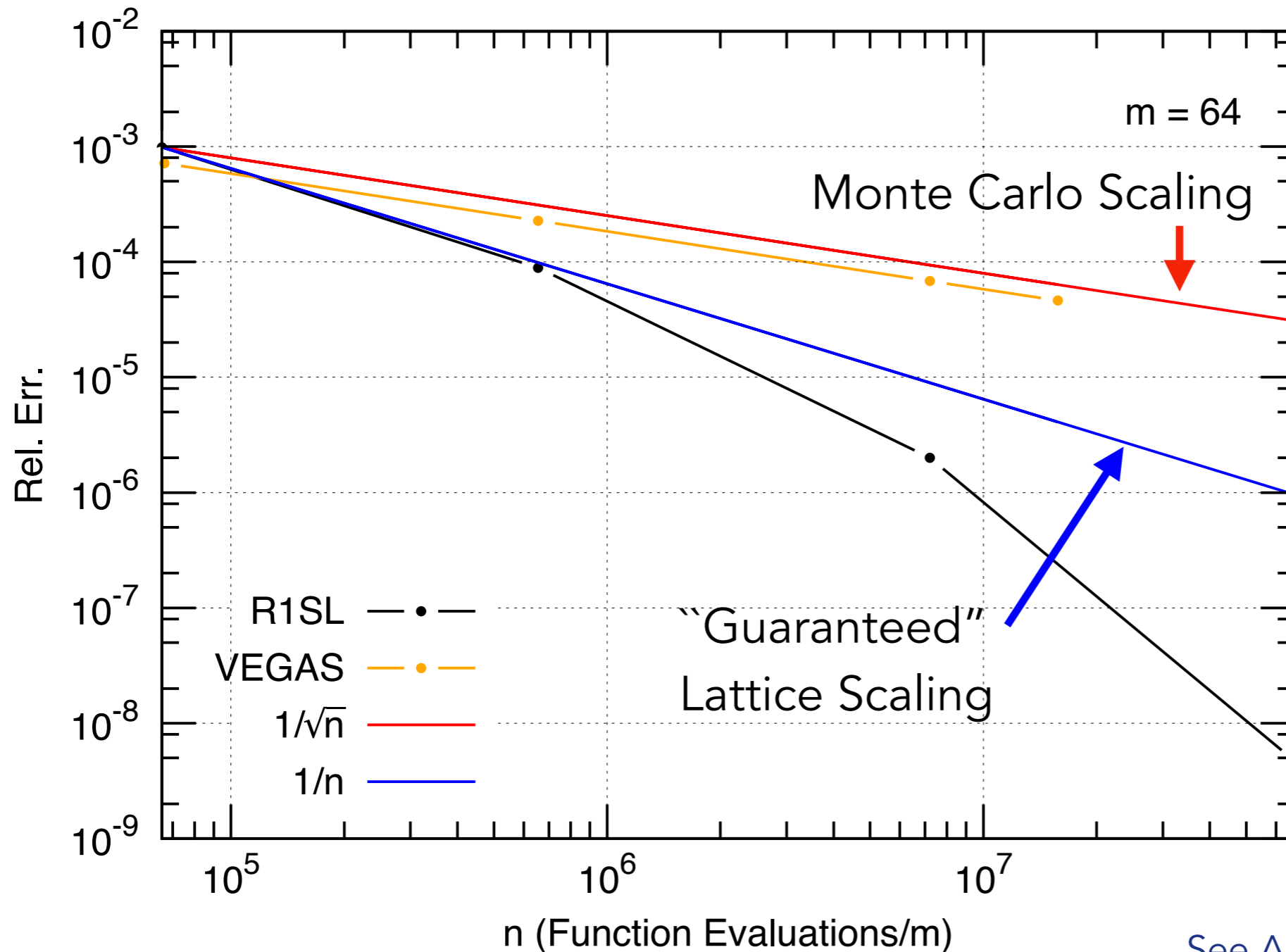


4 Shifts

Typically 10-50 shifts, production run: 20 shifts

R1SL: Algorithm Performance

Example: Rel. Err. of one sector of sector decomposed loop integral



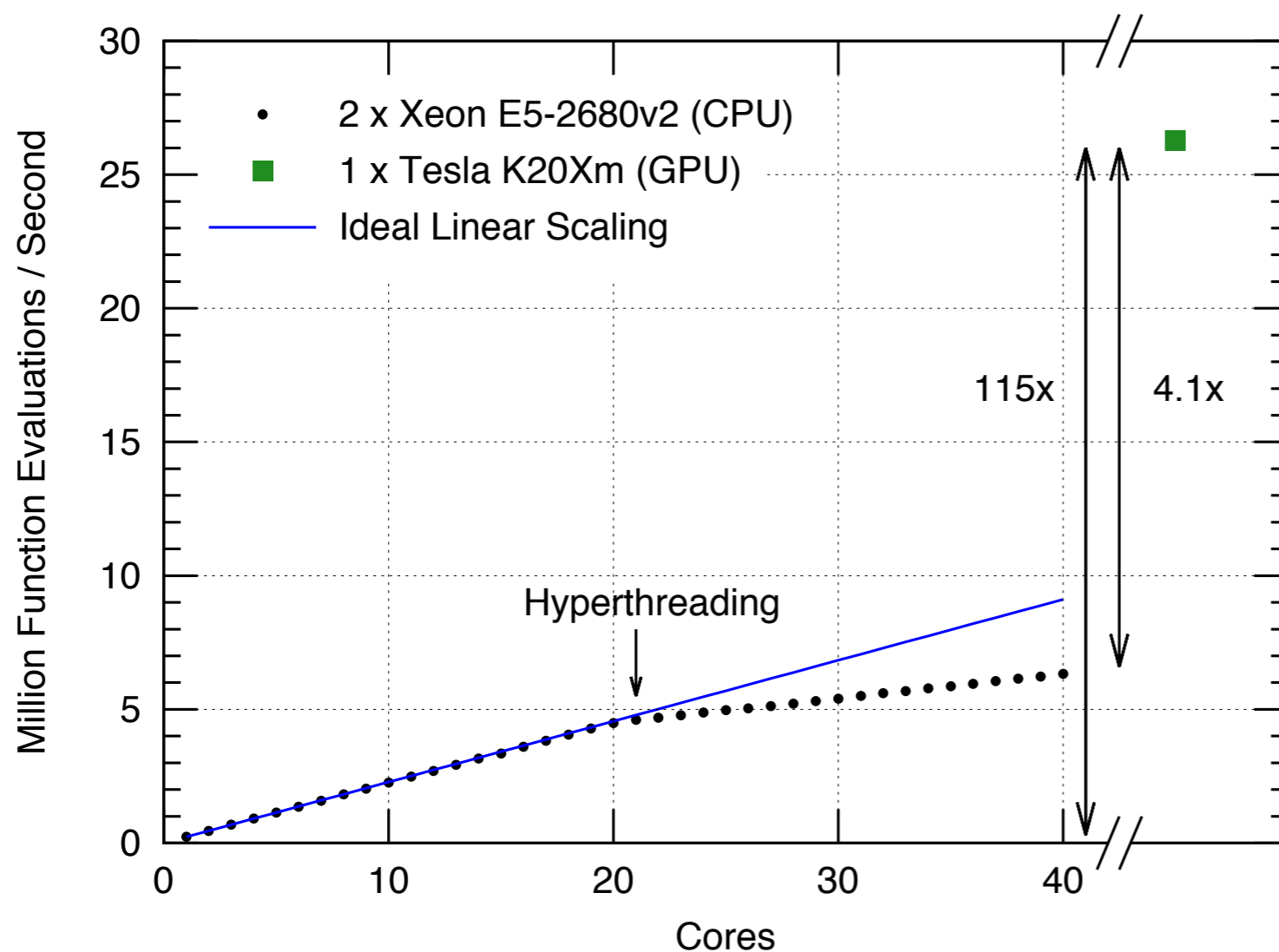
6 dimensional
numerical
integral

See Also: Li, Wang, Yan, Zhao 15

R1SL: Implementation Performance

Accuracy limited primarily by number of function evaluations

Implemented in OpenCL 1.1 for CPU & GPU, generate points on GPU/
CPU core, sum blocks of points (reduce memory usage/transfers)



2 CPUs (20 Cores + HT)

1 GPU

n	CPU (s)	GPU(s)	C/G
655357	6.63	1.60	4.1
7208951	72.3	16.4	4.4
67264993	674.2	152.2	4.4

Current Experimental Limits

Decay Ch.	B.R.	95% Excl.	Analysis ($[fb^{-1}]$, \sqrt{s} [TeV])
$b\bar{b}b\bar{b}$	33%	$< 29 \cdot \sigma_{SM}$	ATLAS-CONF-2016-017 (3.2,13) ATLAS-CONF-2016-049 (13.3,13)
$b\bar{b}WW$	25%	—	—
$b\bar{b}\tau\tau$	7.3%	$< 200 \cdot \sigma_{SM}$	CMS PAS HIG-16-012 (2.7,13) CMS PAS HIG-16-028 (12.9,13) CMS PAS HIG-15-013 (18.3,8)
$b\bar{b}ZZ$	3.0%	—	—
$WW\tau\tau$	2.71%	—	—
$WWZZ$	1.13%	—	—
$b\bar{b}\gamma\gamma$	0.26%	$< 3.9pb$ $< 74 \cdot \sigma_{SM}$	ATLAS-CONF-2016-004 (3.2,13) CMS-HIG-13-032 (19.7,8)
$\gamma\gamma\gamma\gamma$	0.001%	—	—
$b\bar{b}VV(\rightarrow l\nu l\nu)$	1.23%	$400 \cdot \sigma_{SM}$	CMS PAS HIG-16-024 (2.3,13)
$\gamma\gamma WW^*(\rightarrow l\nu jj)$	—	$< 25pb$	ATLAS-CONF-2016-071 (13.3,13)
Comb Ch.	—	$< 70 \cdot \sigma_{SM}$	ATLAS arXiv:1509.04670v2 (20.3,8)

Future Experimental Prospects

HL-LHC (14 TeV)

ATLAS+CMS $b\bar{b}\gamma\gamma$ + $b\bar{b}\tau\tau$: Expected significance 1.9 sigma
[CERN-LHCC-2015-10](#)

ATLAS $b\bar{b}\gamma\gamma$: Signal significance 1.3 sigma [ATL-PHYS-PUB-2014-019](#)

ATLAS $b\bar{b}\tau\tau$: Signal significance 0.6 sigma [ATL-PHYS-PUB-2015-046](#)

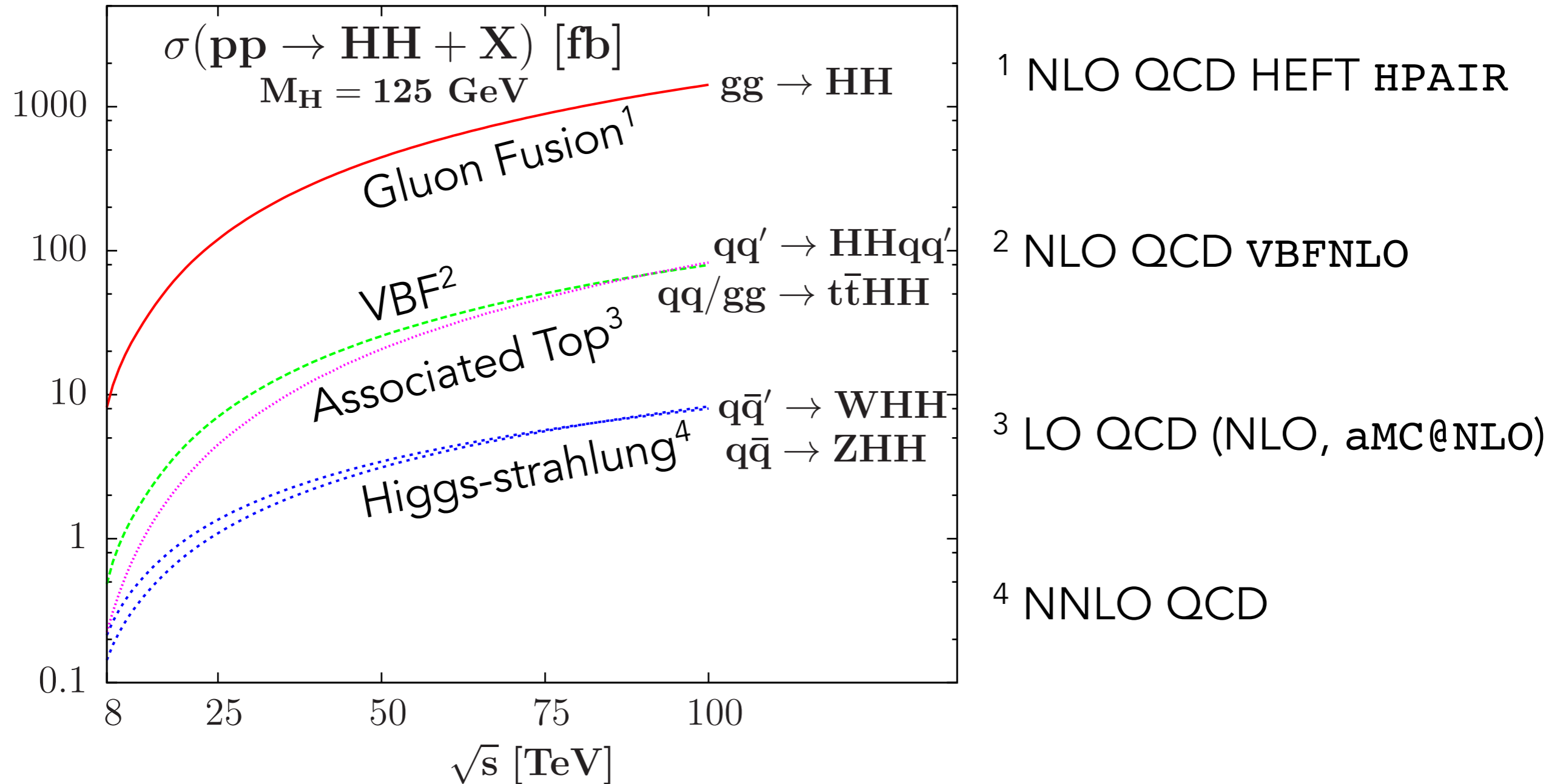
FCC (100 TeV)

This rate is expected to provide a clear signal in the $HH \rightarrow (b\bar{b})(\gamma\gamma)$ channel and to allow determination of λ_{3H} with an accuracy of 30–40% with a luminosity of 3 ab^{-1} , and of 5–10% with a luminosity of 30 ab^{-1} [497–499]. A rare decay channel which is potentially interesting is $HH \rightarrow (b\bar{b})(ZZ) \rightarrow (b\bar{b})(4l)$, with a few expected signal events against $\mathcal{O}(10)$ background events at 3 ab^{-1} [500].

[arXiv:1607.01831](#)

Production Channels (II)

$$\sigma(pp \rightarrow HH + X) \sim \frac{1}{1000} \sigma(pp \rightarrow H + X)$$



Resonant Production

YR4 details two benchmark scenarios for initial study

Higgs Singlet Model

$$V = -m^2 \Phi^\dagger \Phi - \mu^2 S^2 + \lambda_1 (\Phi^\dagger \Phi)^2 + \lambda_2 S^4 + \lambda_3 \Phi^\dagger \Phi S^2$$

$$\Phi^T = (\phi^+, \tilde{\phi}_0 = \frac{\phi_0 + v}{\sqrt{s}})$$
$$S = \frac{s + \langle S \rangle}{\sqrt{2}}$$

Large $\mathcal{O}(20 - 30\%)$ $H \rightarrow hh$

Cross-section can be enhanced by up to 10-20x

2 Higgs Doublet Model (2HDM)

2 neutral scalars $\rightarrow h^0, H^0, A, H^+, H^- \leftarrow$ 2 charged Higgs
 \uparrow
Pseudoscalar

Behaviour strongly depends on the scenario

Hespel, López-Val, Vryonidou 14

Integral Families

tensor integrals: scalar products \rightarrow inverse propagators

Slide: Matthias Kerner

l.i. scalar products:

$$S = \frac{l(l+1)}{2} + lm \quad \begin{array}{l} l = 2 : \quad \# \text{ loops} \\ m = 3 : \quad \# \text{ l.i. external momenta} \end{array} \Rightarrow S = 9$$

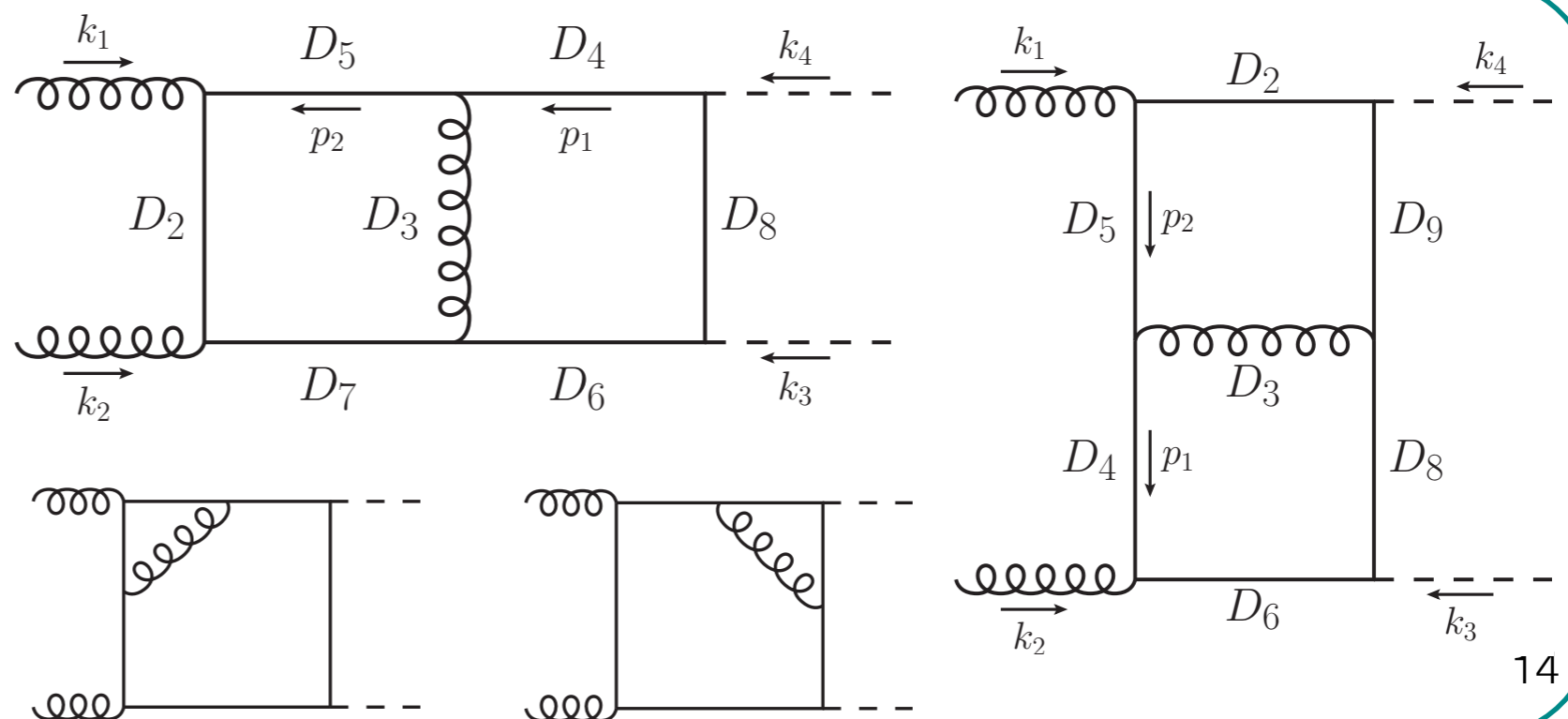
\rightarrow integral families with 9 propagators

\rightarrow general loop integral:

$$I_{\nu_1, \dots, \nu_9}^{\text{fam}_j} = \int d^d p_1 \int d^d p_2 \frac{1}{D_1^{\nu_1} D_2^{\nu_2} \dots D_9^{\nu_9}} \quad \nu_i \in \mathbb{Z}$$

planar family 1:

$$\begin{aligned} D_1 &= p_1^2 - m_t^2 \\ D_2 &= p_2^2 - m_t^2 \\ D_3 &= (p_1 - p_2)^2 \\ D_4 &= (p_1 + k_1)^2 - m_t^2 \\ D_5 &= (p_2 + k_1)^2 - m_t^2 \\ D_6 &= (p_1 - k_2)^2 - m_t^2 \\ D_7 &= (p_2 - k_2)^2 - m_t^2 \\ D_8 &= (p_1 - k_2 - k_3)^2 - m_t^2 \\ D_9 &= (p_2 - k_2 - k_3)^2 - m_t^2 \end{aligned}$$



Integral Families

tensor integrals: scalar products \rightarrow inverse propagators

Slide: Matthias Kerner

l.i. scalar products:

$$S = \frac{l(l+1)}{2} + lm$$

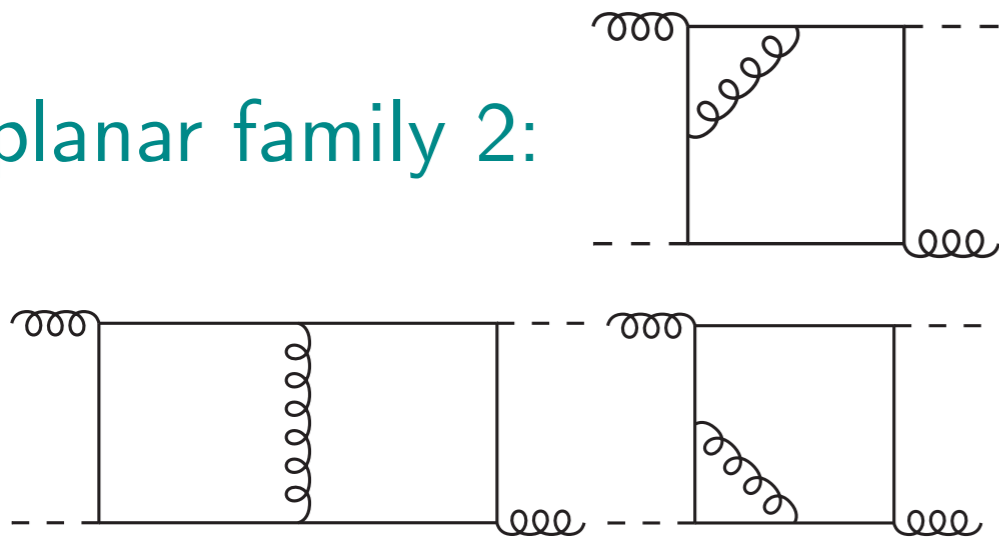
$l = 2$: # loops

$m = 3$: # l.i. external momenta

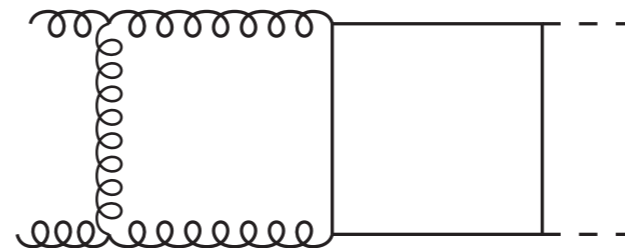
$$\Rightarrow S = 9$$

\rightarrow integral families with 9 propagators

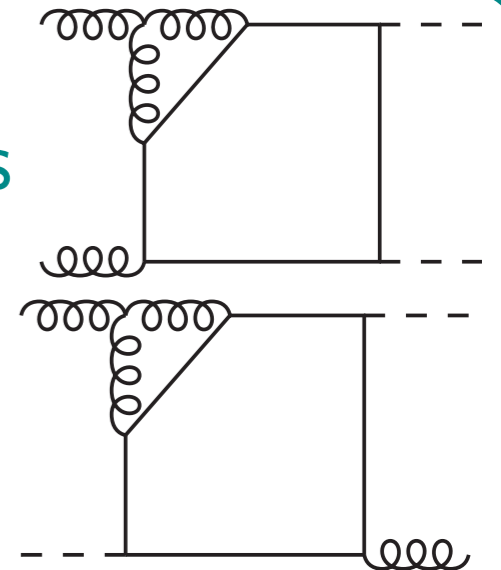
planar family 2:



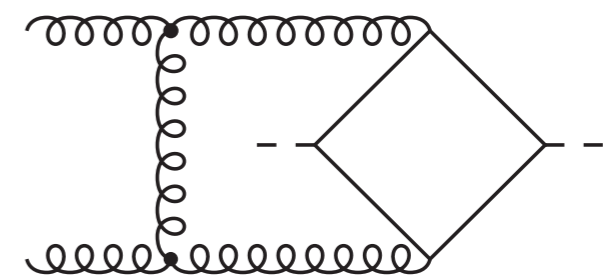
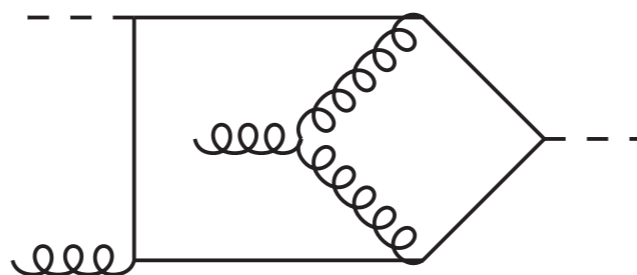
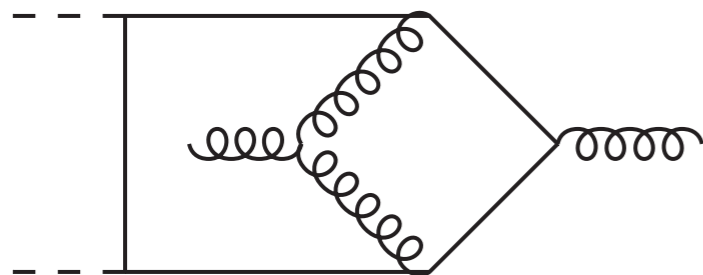
planar family 3:



planar families 4/5:



3 non-planar families:



Form Factor Decomposition (II)

$$T_1^{\mu\nu} = g^{\mu\nu} - \frac{p_2^\mu p_1^\nu}{p_1 \cdot p_2} \qquad p_T^2 = \frac{ut - m_H^4}{s}$$

$$T_2^{\mu\nu} = g^{\mu\nu} + \frac{m_H^2 p_2^\mu p_1^\nu}{p_T^2 p_1 \cdot p_2} - \frac{2p_1 \cdot p_3 p_2^\mu p_3^\nu}{p_T^2 p_1 \cdot p_2} - \frac{2p_2 \cdot p_3 p_3^\mu p_1^\nu}{p_T^2 p_1 \cdot p_2} + \frac{2p_3^\mu p_3^\nu}{p_T^2}$$

Glover, van der Bij 88

Projectors (CDR $D = 4 - 2\epsilon$):

$$P_1^{\mu\nu} = \frac{1}{4} \frac{D-2}{D-3} T_1^{\mu\nu} - \frac{1}{4} \frac{D-4}{D-3} T_2^{\mu\nu}$$

$$P_2^{\mu\nu} = -\frac{1}{4} \frac{D-4}{D-3} T_1^{\mu\nu} + \frac{1}{4} \frac{D-2}{D-3} T_2^{\mu\nu}$$

**Same Basis as
amplitude**

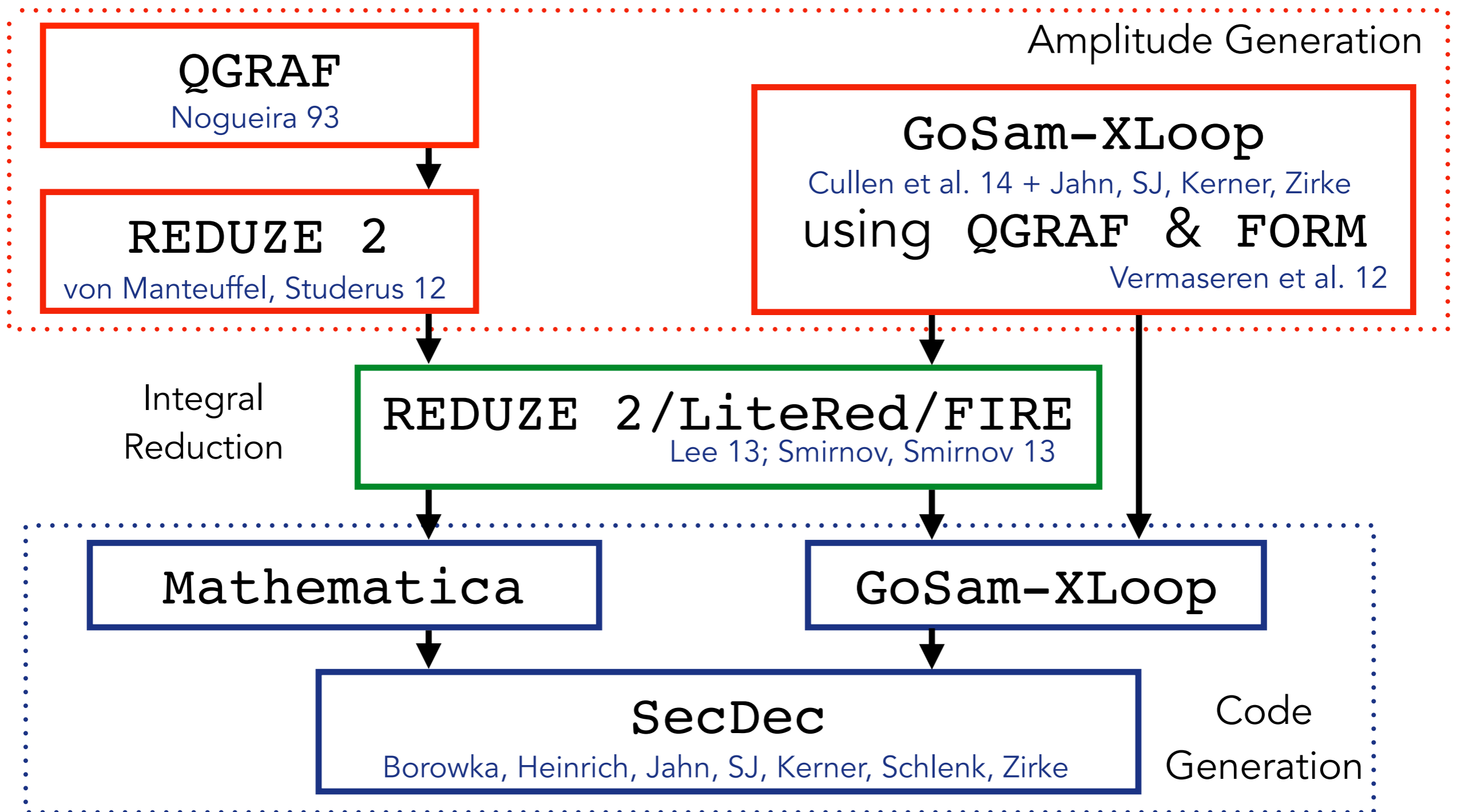
Compute:

$$P_1^{\mu\nu} \mathcal{M}_{\mu\nu} = F_1(\hat{s}, \hat{t}, m_h^2, m_t^2, D)$$

$$P_2^{\mu\nu} \mathcal{M}_{\mu\nu} = F_2(\hat{s}, \hat{t}, m_h^2, m_t^2, D)$$

Virtual MEs: Tool Chain

Partial cross-check: 2 Implementations



Master Integrals

Known Analytically:

Spira, Djouadi et al. 93, 95;
 Bonciani, P. Mastrolia 03,04;
 Anastasiou, Beerli et al. 06;

3-point, 1 off-shell leg
 HPLs

Gehrmann, Guns, Kara 15

3-point, 2 off-shell legs
 Generalized HPLs, 12 Letters

Numeric Evaluation:

Up to 4-point,
 4 scales s, t, m_T^2, m_H^2
 SecDec

Numerical Master Integrals

To evaluate Master Integrals we use **SecDec** which implements Sector Decomposition

Collaboration: Borowka, Heinrich, Jahn, SJ, Kerner, Schlenk, Zirke

Completely automated procedure

Sector Decomposition

1) Feynman Parametrise integral and compute momentum integrals

$$G = (-1)^{N_\nu} \frac{\Gamma(N_\nu - LD/2)}{\prod_{j=1}^N \Gamma(\nu_j)} \int_0^\infty \prod_{j=1}^N dx_j x_j^{\nu_j-1} \delta(1 - \sum_{i=1}^N x_i) \frac{\mathcal{U}^{N_\nu - (L+1)D/2}(\vec{x})}{\mathcal{F}^{N_\nu - LD/2}(\vec{x}, s_{ij})}$$

Here \mathcal{U}, \mathcal{F} are 1st, 2nd Symanzik Polynomials

We have exchanged L momentum integrals for N parameter integrals

Sector Decomposition

2) After integrating out δ we are faced with integrals of the form:

$$G_i = \int_0^1 \left(\prod_{j=1}^{N-1} dx_j x_j^{\nu_j - 1} \right) \frac{\mathcal{U}_i(\vec{x})^{\text{expo}\mathcal{U}(\epsilon)}}{\mathcal{F}_i(\vec{x}, s_{ij})^{\text{expo}\mathcal{F}(\epsilon)}} \leftarrow \text{Powers depending on } \epsilon$$

↑
Polynomials in F.P

Which may contain overlapping singularities which appear when several $x_j \rightarrow 0$ simultaneously (corresponding to UV/IR singularities)

Sector decomposition maps each integral into integrals of the form:

$$G_{ik} = \int_0^1 \left(\prod_{j=1}^{N-1} dx_j x_j^{a_j - b_j \epsilon} \right) \frac{\mathcal{U}_{ik}(\vec{x})^{\text{expo}\mathcal{U}(\epsilon)}}{\mathcal{F}_{ik}(\vec{x}, s_{ij})^{\text{expo}\mathcal{F}(\epsilon)}}$$

↑

$$\mathcal{U}_{ik}(\vec{x}) = 1 + u(\vec{x})$$

$$\mathcal{F}_{ik}(\vec{x}) = -s_0 + f(\vec{x}) \leftarrow u(\vec{x}), f(\vec{x}) \text{ have no constant term}$$

Singularity structure can be read off

Sector Decomposition (II)

One technique **Iterated Sector Decomposition** repeat:

Binoth, Heinrich 00

$$\begin{aligned}
 & \int_0^1 dx_1 \int_0^1 dx_2 \frac{1}{(x_1 + x_2)^{2+\epsilon}} \quad \leftarrow \text{Overlapping singularity for } x_1, x_2 \rightarrow 0 \\
 &= \int_0^1 dx_1 \int_0^1 dx_2 \frac{1}{(x_1 + x_2)^{2+\epsilon}} (\theta(x_1 - x_2) + \theta(x_2 - x_1)) \\
 &= \int_0^1 dx_1 \int_0^{x_1} dx_2 \frac{1}{(x_1 + x_2)^{2+\epsilon}} + \int_0^1 dx_2 \int_0^{x_2} dx_1 \frac{1}{(x_1 + x_2)^{2+\epsilon}} \\
 &= \int_0^1 dx_1 \int_0^1 dt_2 \frac{x_1}{(x_1 + x_1 t_2)^{2+\epsilon}} + \int_0^1 dx_2 \int_0^1 dt_1 \frac{x_2}{(x_2 t_1 + x_2)^{2+\epsilon}} \\
 &= \int_0^1 dx_1 \int_0^1 dt_2 \frac{x_1^{-1-\epsilon}}{(1 + t_2)^{2+\epsilon}} + \int_0^1 dx_2 \int_0^1 dt_1 \frac{x_2^{-1-\epsilon}}{(t_1 + 1)^{2+\epsilon}} \quad \leftarrow \text{Singularities factorised}
 \end{aligned}$$

If this procedure terminates depends on order of decomposition steps

An alternative strategy **Geometric Sector Decomposition** always terminates; both strategies are implemented in SecDec.

Kaneko, Ueda 10; See also: Bogner, Weinzierl 08; Smirnov, Tentyukov 09

Sector Decomposition (III)

3) Expand in ϵ (simple case $a = -1$):

$$\int_0^1 dx x^{-1-b\epsilon} g(x) = \frac{g(0)}{-b\epsilon} + \int_0^1 dx x^{-b\epsilon} \left[\frac{g(x) - g(0)}{x} \right]$$

Poles (arrow pointing to $-b\epsilon$)

Finite (arrow pointing to the bracketed term)

Note: 'subtraction' of $g(0)$ (arrow pointing to $g(x) - g(0)$)

By Definition: $g(0) \neq 0$, $g(0)$ finite

4) Numerically integrate

SecDec supports: numerators, inverse propagators, "dots", physical kinematics, arbitrary loops & legs (within reason)

Soper 00; Nagy, Soper 06;
Borowka 14

Key Point: Sector Decomposed integrals can be expanded in ϵ and numerically integrated

SecDec as a Library

Single program to compute **all** coefficients & integrals to obtain **amplitude** to given accuracy

desired precision

list of GPUs & CPUs

```
Amplitude si(epsrel,devinds,crossings);
```

```
// coeffs/coeff1.cpp
```

```
si.addTerm(
```

```
    string("ReduzeF1L2_230000010ord0"),  
    ReduzeF1L2_230000010ord0func(),  
    crossing,  
    &ReduzeF1L2_230000010ord0Integrand,  
    &ReduzeF1L2_230000010ord0findoptlam,  
    ReduzeF1L2_230000010ord0ndim(),  
    params,  
    termCoeff1  
);
```

name & reference to
integrand to integrate

$(\hat{s}, \hat{t}, m_t^2, m_h^2)$

vector of coefficients
 $C_{1,-2}, C_{1,-1}, \dots$ for all Form
Factors, evaluated at this
phase-space point

```
// coeffs/coeff204.cpp
```

```
si.addTerm(
```

```
    string("ReduzeF3L2diminc2_131010100ord1"),  
    ReduzeF3L2diminc2_131010100ord1func(),  
    crossing,  
    &ReduzeF3L2diminc2_131010100ord1Integrand,  
    &ReduzeF3L2diminc2_131010100ord1findoptlam,  
    ReduzeF3L2diminc2_131010100ord1ndim(),  
    params,  
    termCoeff2  
);
```

Find contour
deformation
(physical region) in
parallel for all
integrals in
amplitude

```
si.optimizeLambda();  
si.integrate();
```

Computes integrals in parallel on GPUs
& CPUs. Dynamically adjusts # points
per sector to reduce amplitude error

Slide:
Tom
Zirke

Approximate top-mass effects at NLO

$$\begin{aligned} \sigma^{NLO}(p) = & \int d\phi_3 \left[(d\sigma^R(p))_{\epsilon=0} - \left(\sum_{\text{dipoles}} d\sigma^{LO}(p) \otimes dV_{\text{dipole}} \right)_{\epsilon=0} \right] \checkmark \\ & + \int d\phi_2 [d\sigma^V(p) + d\sigma^{LO}(p) \otimes \mathbf{I}]_{\epsilon=0} \\ & + \int_0^1 dx \int d\phi_2 [d\sigma^{LO}(xp) \otimes (\mathbf{P} + \mathbf{K})(x)]_{\epsilon=0} \checkmark \end{aligned}$$

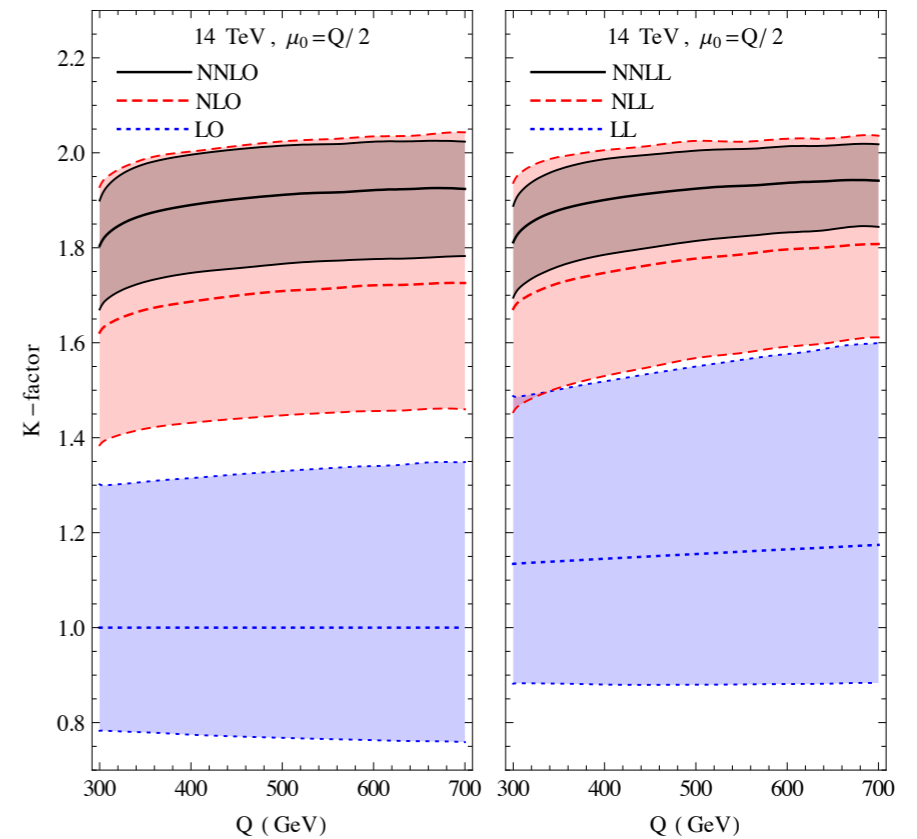
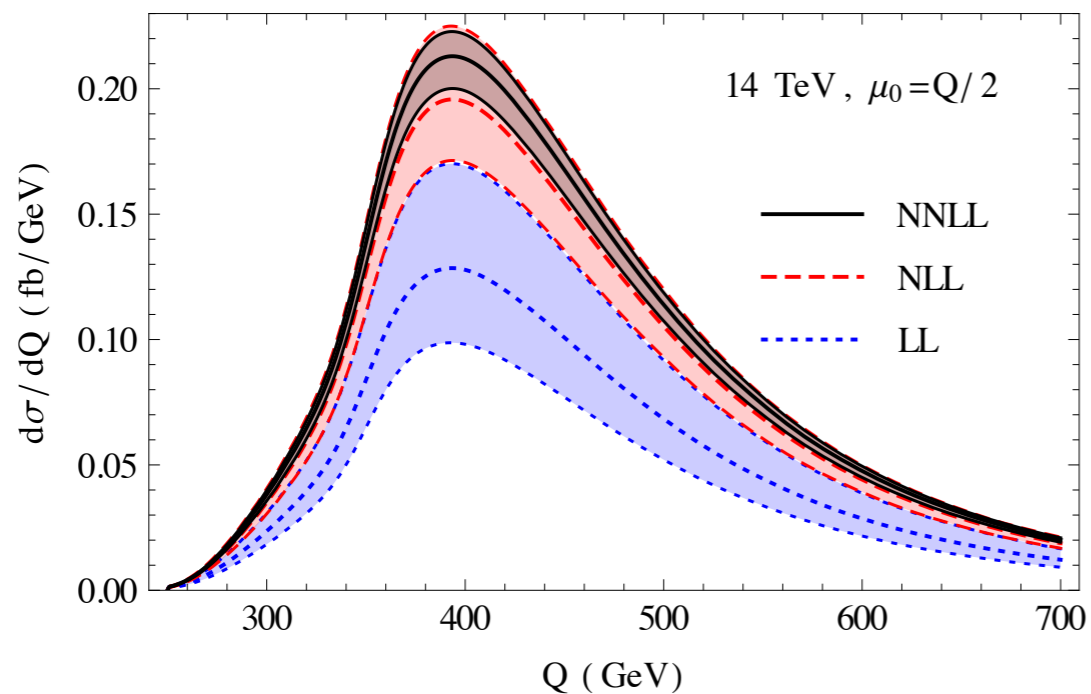
$$\begin{aligned} d\sigma^V + d\sigma^{LO}(\epsilon) \otimes \mathbf{I} & \approx d\sigma_{\text{exp},N}^V \frac{d\sigma^{LO}(\epsilon)}{d\sigma_{\text{exp},N}^{LO}(\epsilon)} + d\sigma^{LO}(\epsilon) \otimes \mathbf{I} \\ & = (d\sigma_{\text{exp},N}^V + d\sigma_{\text{exp},N}^{LO}(\epsilon) \otimes \mathbf{I}) \frac{d\sigma^{LO}(\epsilon)}{d\sigma_{\text{exp},N}^{LO}(\epsilon)} \\ & = (d\sigma_{\text{exp},N}^V + d\sigma_{\text{exp},N}^{LO}(\epsilon) \otimes \mathbf{I}) \frac{d\sigma^{LO}(\epsilon=0)}{d\sigma_{\text{exp},N}^{LO}(\epsilon=0)} + \mathcal{O}(\epsilon) \end{aligned}$$

$$d\sigma_{\text{exp},N} = \sum_{k=0}^N d\sigma^{(k)} \left(\frac{\Lambda}{m_t} \right)^{2k}$$

$$\Lambda \in \{ \sqrt{s}, \sqrt{t}, \sqrt{u}, m_h \}$$

- full real-emission matrix elements and dipoles
- virtual corrections as asymptotic expansion in $1/m_t^2$ with `q2e/exp` [Harlander, Seidensticker, Seidensticker] + `Reduze` [von Manteuffel, Studerus] + `matad` [Steinhauser]
- not directly comparable with [Grigo, Hoff, Steinhauser], (real radiation treated differently, expansion parameter $(m_H/m_t)^2$)

HEFT NNLO + NNLL



de Florian, Mazzitelli 15

$\mu_0 = Q$	NNLO (fb)	scale unc. (%)	NNLL (fb)	scale unc. (%)	PDF unc. (%)	PDF+ α_S unc. (%)
8 TeV	9.92	+9.3 – 10	10.8	+5.4 – 5.9	+5.6 – 6.0	+9.3 – 9.2
13 TeV	34.3	+8.3 – 8.9	36.8	+5.1 – 6.0	+4.0 – 4.3	+7.7 – 7.5
14 TeV	40.9	+8.2 – 8.8	43.7	+5.1 – 6.0	+3.8 – 4.0	+7.5 – 7.3
33 TeV	247	+7.1 – 7.4	259	+5.0 – 6.1	+2.2 – 2.8	+6.1 – 6.1
100 TeV	1660	+6.8 – 7.1	1723	+5.2 – 6.1	+2.1 – 3.0	+5.7 – 5.8
$\mu_0 = Q/2$	NNLO (fb)	scale unc. (%)	NNLL (fb)	scale unc. (%)	PDF unc. (%)	PDF+ α_S unc. (%)
8 TeV	10.8	+5.7 – 8.5	11.0	+4.0 – 5.6	+5.8 – 6.1	+9.6 – 9.3
13 TeV	37.2	+5.5 – 7.6	37.4	+4.2 – 5.8	+4.1 – 4.3	+7.8 – 7.6
14 TeV	44.2	+5.5 – 7.6	44.5	+4.2 – 5.9	+3.9 – 4.1	+7.6 – 7.4
33 TeV	264	+5.3 – 6.6	265	+4.6 – 6.1	+2.4 – 2.7	+6.3 – 6.1
100 TeV	1760	+5.3 – 6.7	1762	+4.9 – 6.4	+2.2 – 3.1	+6.2 – 7.0

G.H.S Top Mass Expansion

